doi.org/10.26434/chemrxiv.12375215.v1

Chemoselectivity Switching through Coupled Equilibria

Ognjen Miljanic, Thamon Puangsamlee

Submitted date: 27/05/2020 • Posted date: 28/05/2020

Citation information: Miljanic, Ognjen; Puangsamlee, Thamon (2020): Chemoselectivity Switching through Coupled Equilibria. ChemRxiv. Preprint. https://doi.org/10.26434/chemrxiv.12375215.v1

Complex mixtures are found in biological and petrochemical feedstocks, and in the primordial soup implicated in the origins of life. Reacting individual compounds within these mixtures is challenging because of the difficulty in controlling the chemoselectivity of such reactions. We show that the selectivity of imine oxidation can be controlled within doubly dynamic combinatorial libraries, wherein two coupled equilibria determine whether the most oxidizable aldehyde precursor is made available to the oxidant or sequestered away from it. Under the slow oxidation conditions, the most electron-rich precursor can traverse the shallow energy landscape and its oxidation product dominates the final mixture. Faster oxidation captures the imine mixture composition, favoring the products derived from electron poorer push-pull imines.

Chemoselectivity Switching through Coupled Equilibria

Thamon Puangsamlee and Ognjen Š. Miljanić*

Department of Chemistry, University of Houston, Houston, Texas 77204-5003, United States

ABSTRACT: Complex mixtures are found in biological and petrochemical feedstocks, and in the primordial soup implicated in the origins of life. Reacting individual compounds within these mixtures is challenging because of the difficulty in controlling the chemoselectivity of such reactions. We show that the selectivity of imine oxidation can be controlled within doubly dynamic combinatorial libraries, wherein two coupled equilibria—those of imine exchange and the diaza-Cope rearrangement—determine whether the most oxidizable aldehyde precursor is made available to the oxidant or sequestered away from it. Under the slow oxidation conditions, the most electron-rich precursor can traverse the shallow energy landscape and its oxidation product dominates the final mixture. Faster oxidation captures the imine mixture composition, favoring the products derived from electron poorer push-pull imines. Intermediate oxidation rates allow the expression of yet the third possible reaction product. These findings suggest that careful tuning of reactant concentrations and the associated reaction rates can engage individual mixture components into selective reactions even in the absence of specific catalysts.

Control of chemoselectivity is among the central problems of synthetic chemistry.[1] Its ramifications range from solving the mysteries of prebiotic chemistry[2] to improving the efficiencies of separations and functionalizations of feedstocks derived from complex petroleum and biomass sources. For a given set of reactants, reaction outcome is controlled by thermodynamic and kinetic factors. Often, they work hand-in-hand: the most stable reaction products also form the fastest. Sometimes, they do not, and such reactions can express either their kinetic (fastest formed) or thermodynamic (most stable) products. Are these two extremes the only options? In this Communication, we show that they are not: in a complex mixture of equilibrating precursors, final reaction product can be switched at well by changing the rate of reagent addition. The key to this behavior is the use of coupled equilibria, in which the products of one reversible reaction act as the substrates for another. Coupled equilibria phenomena[3] have vast relevance to pollution, climate change,[4] ocean acidification,[5] and metabolic pathways.[6] Complex coupled equilibria often give rise to systems-level and emergent phenomena.[7]

Our studies of irreversible reactions operating on imine dynamic combinatorial libraries (DCLs)[8] have shown that such "messy" precursor mixtures can still be chemoselectively functionalized. As one DCL component reacts the fastest in an irreversible reaction, other library members equilibrate to produce more of it. The net result is the high-yielding functionalization of the most reactive DCL member, which is amplified at the expense of the less reactive members.[9] Applied iteratively, such amplification leads to kinetic self-sorting[10] of the DCL into just a handful of fast-reacting components. Self-sorting hinges on the applicability of the Curtin-Hammett principle,[11] which implies much faster rate of the DCL equilibration compared to the irreversible removal reaction. In such a scenario, relative stabilities of different imines have no bearing on the final reaction products: it is only the relative rates of that irreversible reaction which determine the chemoselectivity. In this study, we manipulated these relative reaction rates, causing a breakdown of the Curtin-Hammett selectivity but in turn revealing a rich reactivity landscape wherein products can be selected by adjusting the rate of the irreversible removal reaction.

Imines formed from 1,2-phenylenediamine (**3**, Scheme 1) and aromatic aldehydes can be oxidized into corresponding benzimidazoles using relatively elemental iodine (I_2). This oxidation is faster for imines formed from electron-rich aldehyde and amine components than for those derived from electron-poor precursors. During our studies of oxidative self-sorting of imines,[12] we noticed that the product distribution could additionally be influenced by the rate of oxidant addition. The reaction of equimolar amounts of 4-nitrobenzaldehyde (**1**), 4-methoxybenzaldehyde (**2**), and **3** generated a mixture of imines **4** and **5**, along with some leftover aldehydes. When this mixture was treated with I_2 as the oxidant, the imines were converted into benzimidazoles **6** and **7**. The ratio of the two products depended on the rate of I_2 addition. If I_2 was added very slowly—over 120 h—the methoxy-substituted **6** constituted 87% of the product mixture. On the other hand, instantaneous (<2 min) I_2 addition resulted in benzimidazole **7** as the dominant product (76%). This selectivity switching could be explained as follows. The intermediate imine mixture has more of the nitro-substituted imine **4**: its push-pull electronic nature means it is both more stable and more quickly formed than the methoxy-substituted **5**. If the oxidation is quick, it captures this composition of imine precursors in the final ratio of benzimidazole products. However, if the oxidation is very slow, the

Scheme 1. Oxidation of the mixture of imines 4 and 5 produces 6 and 7 in a ratio dependent on the rate of the I_2 addition.

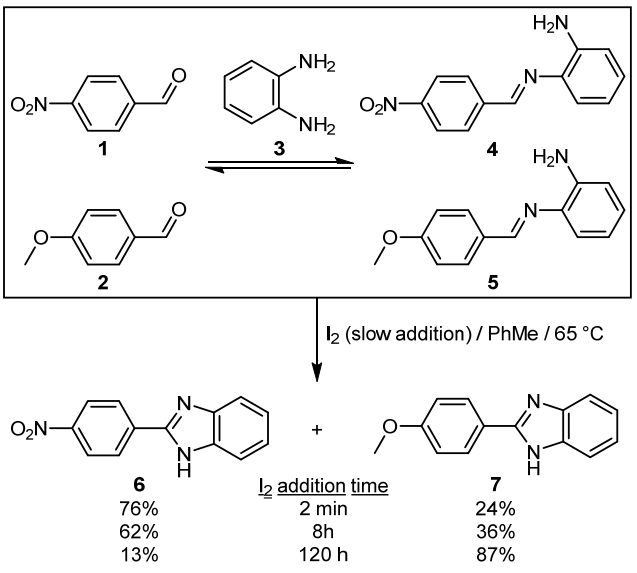

dynamic imine mixture has enough time to continuously replenish the electron-rich imine **5** which is being preferentially consumed by its faster oxidation. Slower to oxidize, **4** instead releases its 1,2-phenylenediamine component to create more of **5**, and the product distribution switches.

Intrigued by this result, we set out to determine whether such selectivity switching could be further controlled. To do so, we designed a dynamic system which operates using two reversible reactions: imine exchange and the diaza-Cope rearrangement of diimines of the general structural type **8** (Scheme 2). Work by Vögtle[13] and others[14] has shown that the diaza-Cope equilibrium favors imines derived from salicylaldehyde (such as **8**) over their rearranged isomers (such as **9**), presumably on account of their greater stabilization by [N···H–O] hydrogen bonding. This equilibrium position means that the salicylaldehyde component (highlighted in red in Scheme 2) can be directly exchanged from its imine **8** by a reaction with **3** to produce oxidizable imine **10**. The more electron-rich 2,4-dimethoxybenzaldehyde (highlighted in blue) cannot directly engage into an oxidation. Instead, **8** must first undergo diaza-Cope rearrangement into the less favored isomer **9** and only then can **9** exchange with **3** to produce the oxidizable imine **11**. Being thus once-removed from the immediate exchange, the electron-rich 2,4-dimethoxybenzaldehyde component must traverse a longer reaction pathway to engage into an oxidation and may not have enough time to do so if oxidation is too fast. Indeed, I_2 addition in 1 min generated effectively only the benzimidazole **12** derived from salicylaldehyde (98:2 selectivity over **13**). As the I_2 addition was slowed down, 2,4-dimethoxybenzaldehyde had enough time to travel across the shallow energy landscape and the mole fraction of its oxidation product (**13**) in the final product mixture increased to 25%, 59%, and finally 76% if I_2 was added over 2 h, 6 h, or 120 h, respectively.

Scheme 2. Oxidation of a mixture of 3, 8, and 9 generates 12 and 13 in a ratio which is dependent on the rate of I_2 addition.

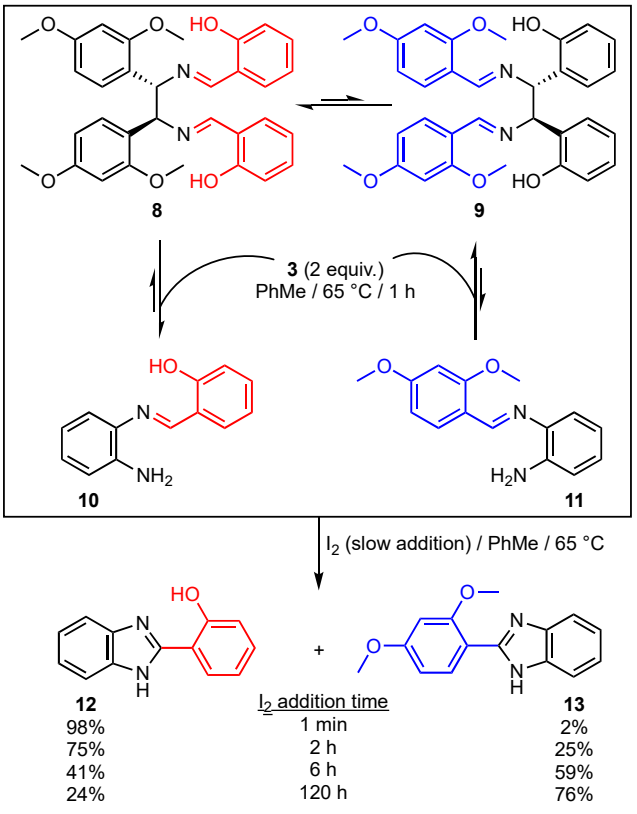

To establish whether this selectivity switching is general, we examined several other diimines analogous to **8** and **9**, which related to each other through diaza-Cope rearrangement (Scheme 3). Salicylaldimines **14a–e** were preferred over their rearranged isomers **15a–e** regardless of the substituents R, and a previous study has shown that the diaza-Cope equilibration slows down for electron-donating R groups.[14a] The addition of **3** once again initiated the increase in the complexity of this dynamic mixture, as imines **10** and **16a–d**/**4** could now be formed, along with partially exchanged species not shown in Scheme 3. Iodine addition then begun, either very slowly or instantaneously. As in the previous experiment, the outcomes of these reactions were dependent on the rate of I_2 addition, but this dependence varied based on the substitution in the starting imines **14**/**15**. In the parent system **14a**/**15a** (R=H), slower addition mildly increased the ratio of product **17a** to product **12**, switching from a relative ratio of 1:4.47 to1:3.29. Selectivity switching observed in Scheme 2 was replicated with the **14b**/**15b** (R=Me) couple; the benzimidazole obtained from the electron-rich **16b** dominated the product mixture under slow addition conditions, while **12**

Scheme 3. Selectivity switching in imine oxidation as a function of substitution and I_2 addition rate.

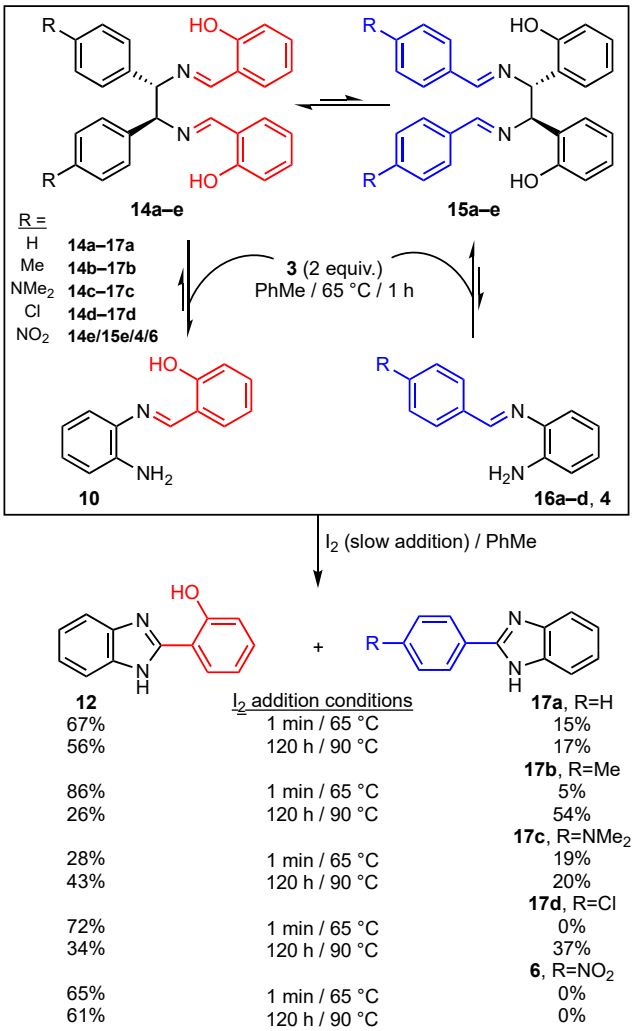

was the main product if I_2 was added instantaneously. In compounds **14c**/**15c**, the result was puzzling: the significantly more electron-rich *para*-*N*,*N*-dimethylamino substituent failed to yield **16c** as the dominant product even at long addition times. Possible explanation for this aberration can be found in the slowdown of the diaza-Cope rearrangement in systems with electron-rich substituents.[14a] This slowing may have effectively shut down the pre-equilibration, making the imine library not dynamic anymore—and the product ratio independent of the I_2 addition rate. The example of **14d**/**15d** (R=Cl) offered another interesting conclusion. As expected, **12** dominated under fast addition conditions, but the switch to **17d** as the major product with slower I_2 addition was surprising at first glance. Tentatively, this behavior can be rationalized as follows. The chlorine substituent in the *para*-position is weakly electron-withdrawing, with a Hammett parameter of +0.23. *Ortho*-substitutents are generally not used in Hammett correlations because of steric effects, but an OH group in a *meta* position has a Hammett value close to that of *para*-Cl: +0.12.[15] Stated differently, the OH group influences the electronics of precursor imines by its electron-donating resonance effect, but also as an electron-withdrawing inductive acceptor. Finally, the electron-withdrawing NO_2 group in **14e**/**15e** led to identical product mixtures regardless of the I_2 addition rate: **12** was the only product, with no **6** observed in either case. Nitro-substituted **4** oxidizes so much slower than **10**, that even allowing extra time for pre-equilibration did not make a difference in the amount of produced **6**.

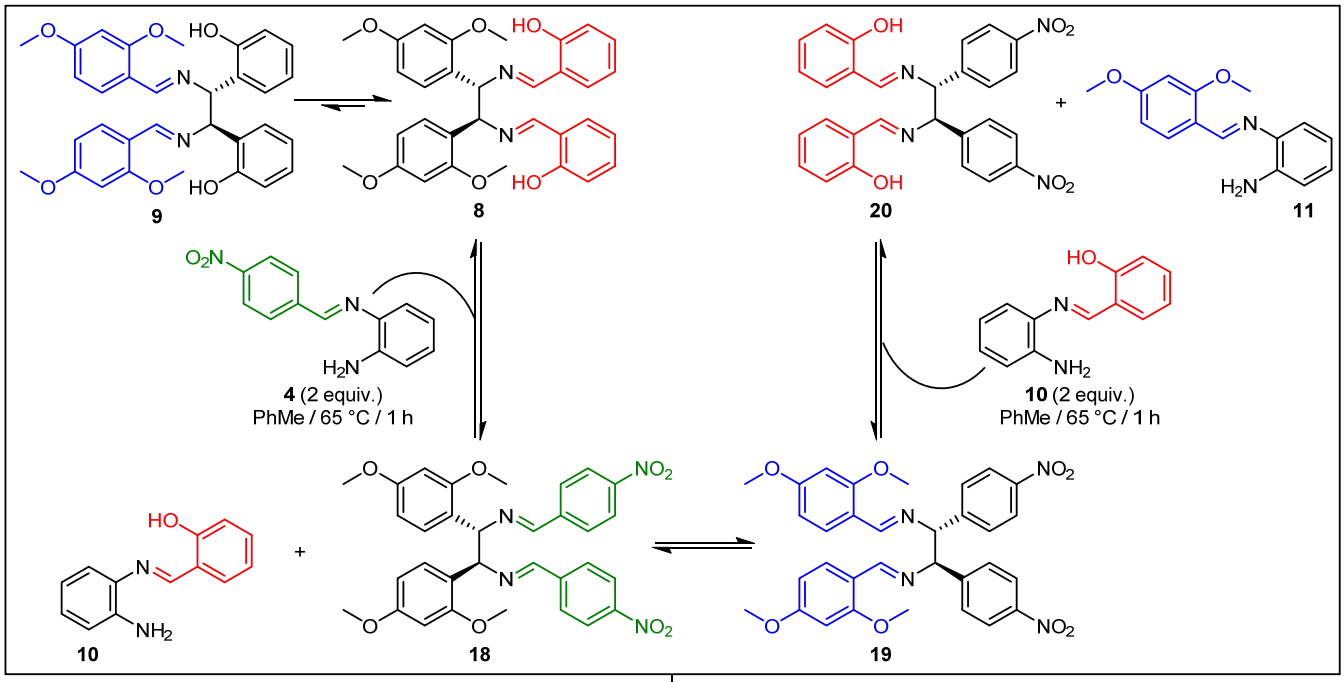

I_2 addition time	13	12	6
1 min	1%	2%	65%
1 h	12%	14%	0%
2 h	12%	25%	0%
3 h	20%	29%	0%
4 h	22%	41%	0%
5 h	22%	14%	0%
6 h	37%	23%	0%
120 h	93%	7%	0%

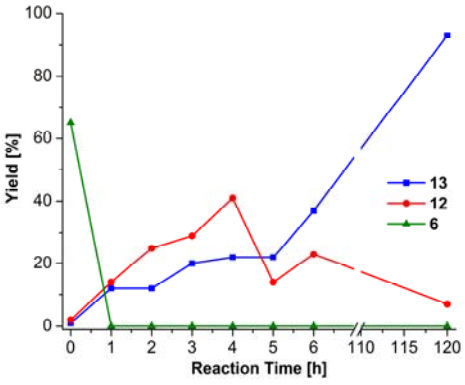

Scheme 4. Three-way switching of chemoselectivity in imine oxidation as a function of I_2 addition rate.

Encouraged by the confirmation of this hypothesis, we speculated that a three-way selectivity switching may be possible as well. The experiments aimed at testing this hypothesis exposed the diaza-Cope precursor **8** not to 1,2-phenylenediamine (**3**), but instead to its imine with 4-nitrobenzaldehyde (**4**). Three oxidation products could be anticipated from such a DCL (Scheme 4). With very fast oxidant addition, imine **4** would have no time to exchange with **8** and would simply oxidize into **6**. If oxidation was slower, the exchange between **8** and **4** was expected to generate **10** and **18** could then be oxidized into **12** faster than the electron-poorer **4**. Finally, if oxidant addition was slower still, diaza-Cope rearrangement of **8** or **18** into **9** or **19** could have occurred. The electron-richest imine **11** could be formed from either of these two latter imines by imine metathesis and its fast oxidation would have produced the third possible product: benzimidazole **13**. A series of experiments confirmed this analysis. Instantaneous addition of I_2 to the reaction mixture produced only benzimidazole **6**, derived from the electron-poorest oxidation precursor **4**. As the oxidation was slowed to 2–4 h, salicylaldehyde-derived **12** dominated the product mixture, with **13** being the minor

product; under these conditions, no **6** was observed. Oxidant addition over 5–120 h led to the generation of **13** as the major product, with **12** eventually forming just 7% of the product mixture.

In conclusion, we have shown that the tuning of relative rates of irreversible and reversible transformations in a DCL can express a variety of its members, ranging from electron-rich to electron-poor. This product selection was accomplished in the absence of any enzyme or synthetic catalysts that could impart selectivity, and the only parameter changed was simply the rate of oxidant addition. These results may offer insights into processes in prebiotic chemistry: multiple components of the "primordial soup" could have selectively reacted under differing spatiotemporal conditions. We have also shown that the diaza-Cope rearrangement can be used as a well-behaved dynamic reaction, thus expanding the arsenal of dynamic combinatorial chemistry.[16] These results suggest that in sufficiently complex mixtures there may in fact exist a continuum of products ranging from absolute thermodynamic minima to a number of local minima, that can all be addressed by sufficiently fine-tuning the rates of reagent addition as well as other simple physical reaction parameters: concentration, pressure, and temperature. We believe that the use of coupled equilibria can allow virtual dialing-in of reactivity in highly complex libraries.

ASSOCIATED CONTENT

Supporting Information. Experimental procedures and copies of ^{1}H NMR spectra. This material is available free of charge via the Internet at http://pubs.acs.org.

AUTHOR INFORMATION

Corresponding Author

* miljanic@uh.edu

Author Contributions

T. P. performed all experiments, and analyzed the results together with O. Š. M. Both authors wrote the manuscript and have given approval to the final version of the manuscript.

ACKNOWLEDGMENT

We acknowledge the support from the Welch Foundation (award E-1768) and the University of Houston. O. Š. M. thanks the Alexander von Humboldt Stiftung for supporting his summer stay at the Ruprecht-Karls-Universität in Heidelberg (Germany), where some of the ideas on which this manuscript is based were conceived.

REFERENCES

1. Shenvi, R. A.; O'Malley, D. P.; Baran, P. S. Chemoselectivity: The Mother of Invention in Total Synthesis. *Acc. Chem. Res.* **2009**, *42*, 530–541
2. Ruiz-Mirazo, K.; Briones, C.; de la Escosura, A. Prebiotic Systems Chemistry: New Perspectives for the Origins of Life. *Chem. Rev.* **2014**, *114*, 285–366
3. (a) Atkins, P.; De Paula, J. Atkins' Physical Chemistry. W. H. Freeman; **2006**, pp. 200–202. (b) Adamson, R.; Parks, P. C. An Experiment in Coupled Equilibria. *J. Chem. Educ.* **1971**, *48*, 120–121.
4. (a) Ferreira, D.; Marshall, J.; Ito, T.; McGee, D. Linking Glacial-Interglacial States to Multiple Equilibria of Climate. *Geophys. Res. Lett.* **2018**, *45*, 9160–9170. (b) Schwartz, S. E.; White, W. H. Solubility Equilibria of the Nitrogen Oxides and Oxyacids in Dilute Aqueous Solution. Gordon and Breach Science Publishers, **1981**. (c) Molina, M. J.; Rowland, F. S. Stratospheric Sink for Chlorofluoromethanes: Chlorine Atom-Catalysed Destruction of Ozone. *Nature* **1974**, *249*, 810–812.
5. (a) Mongin, M.; Baird, M.; Tilbrook, B.; Matear, R. J.; Lenton, A.; Herzfeld, M.; Wild-Allen, K.; Skerratt, J.; Margvelashvili, N.; Robson, B. J.; Duarte, C. M.; Gustafsson, M. S. M.; Ralph, P. J.; Steven, A. D. L. The Exposure of the Great Barrier Reef to Ocean Acidification. *Nat. Commun.* **2016**, *7*, doi.org/10.1038/ncomms10732. (b) Hoegh-Guldberg, O.; Mumby, P. J.; Hooten, A. J.; Steneck, R. S.; Greenfield, P.; Gomez, E.; Harvell, C. D.; Sale, P. F.; Edwards, A. J.; Caldeira, K.; Knowlton, N.; Eakin, C. M.; Iglesias-Prieto, R.; Muthiga, N.; Bradbury, R. H.; Dubi, A.; Hatziolos M. E. Coral Reefs Under Rapid Climate Change and Ocean Acidification. *Science* **2007**, *318*, 1737–1742. (c) McNeil, B. I.; Matear, R. J. Climate Change Feedbacks on Future Oceanic Acidification. *Tellus B* **2007**, *59*, 191–198.
6. www.genome.ad.jp/kegg. Last accessed on May 20, 2020.
7. (a) Miljanić, O. Š. Small-Molecule Systems Chemistry. *Chem.* **2017,** *2*, 502–524. (b) Mattia, E.; Otto, S. Supramolecular Systems Chemistry. *Nat. Nanotech.* **2015**, *10*, 111–119. (c) Peyralans, J. J. P.; Otto, S. Recent Highlights in Systems Chemistry. *Curr. Opin. Chem. Biol.* **2009**, *13*, 705–713. (d) Ludlow, R. F.; Otto, S. Systems Chemistry. *Chem. Soc. Rev.* **2008**, *37*, 101–108.
8. (a) Reek, J. N. H.; Otto, S. Dynamic Combinatorial Chemistry; Wiley-VCH: Weinheim, Germany, **2010**. (b) Corbett, P. T.; Leclaire, J.; Vial, L.; West, K. R.; Wietor, J.-L.; Sanders, J. K. M.; Otto, S. Dynamic Combinatorial Chemistry. *Chem. Rev.* **2006**, *106*, 3652–3711. (c) Rowan, S. J.; Cantrill, S. J.; Cousins, G. R. L.; Sanders, J. K. M.; Stoddart, J. F. Dynamic Covalent Chemistry. *Angew. Chem. Int. Ed.* **2002**, *41*, 898–952. (d) Belowich, M. E.; Stoddart, J. F. Dynamic Imine Chemistry. *Chem. Soc. Rev.* **2012,** *41*, 2003–2024
9. (a) Aymeab, J.-F.; Lehn, J.-M. Self-sorting of Two Imine-based Metal Complexes: Balancing Kinetics and Thermodynamics in Constitutional Dynamic Networks. *Chem. Sci.* **2020**, *11*, 1114–1121. (b) He, M.; Lehn, J.-M. Time-Dependent Switching of Constitutional Dynamic Libraries and Networks from Kinetic to Thermodynamic Distributions. *J. Am. Chem. Soc.* **2019**, *141*, 18560-18569. (c) Osypenko, A.; Dhers, S.; Lehn, J.-M. Pattern Generation and Information Transfer through a Liquid/Liquid Interface in 3D Constitutional Dynamic Networks of Imine Ligands in Response to Metal Cation Effectors. *J. Am. Chem. Soc.* **2019**, *141*, 12724–12737. (d) Hafezi, N.; Lehn. J.-M. Adaptation of Dynamic Covalent Systems of Imine Constituents to Medium Change by Component Redistribution under Reversible Phase Separation. *J. Am. Chem. Soc.* **2012**, *134*, 12861–12868.
10. (a) He, Z.; Jiang, W.; Schalley, C. A. Integrative Self-Sorting: A Versatile Strategy for the Construction of Complex Supramolecular Architecture. *Chem. Soc. Rev.* **2015**, *44*, 779–789. (b) Ji, Q.; Lirag, R. C.; Miljanić, O. Š. Kinetically Controlled Phenomena in Dynamic Combinatorial Libraries. *Chem. Soc. Rev.* **2014**, *43*, 1873–1884. (c) Safont-Sempere, M. M.; Fernández, G.; Würthner, F. Self-Sorting Phenomena in Complex Supramolecular Systems. *Chem. Rev.* **2011**, *111*, 5784–5814. (d) Osowska, K.; Miljanić, O. Š. Kinetic and Thermodynamic Self-Sorting in Synthetic Systems. *Synlett* **2011**, 1643–1648.
11. Seeman, J. I. Effect of Conformational Change on Reactivity in Organic Chemistry. Evaluations, Applications, and Extensions of Curtin-Hammett Winstein-Holness Kinetics. *Chem. Rev.* **1983**, *83*, 83–134.
12. (a) Osowska, K.; Miljanić, O. Š. Oxidative Kinetic Self-Sorting of a Dynamic Imine Library. *J. Am. Chem. Soc.* **2011**, *133*, 724–727. See also: (b) Osowska, K.; Miljanić, O. Š. Self-Sorting of Dynamic Imine Libraries during Distillation. *Angew. Chem. Int. Ed.* **2011**, *50*, 8345–8349. (c) Ji, Q.; Miljanić, O. Š. Distillative Self-Sorting of Dynamic Ester Libraries. *J. Org. Chem.* **2013**, *78*, 12710–12716. (d) Hsu, C.-W.; Miljanić, O. Š. Adsorption-Driven Self-Sorting of Dynamic Imine Libraries. *Angew. Chem. Int. Ed.* **2015**, *54*, 2219–2222. (e) Hsu, C.-W.; Miljanić, O. Š. Kinetically Controlled Simplification of a Multiresponsive [10×10] Dynamic Imine Library. *Chem. Commun.* **2016**, *52*, 12357–12359.

13. Vögtle, F.; Goldschmitt, E. Die Diaza-Cope-Umlagerung. *Chem. Ber.* **1976**, *109*, 1–40.

14. (a) Lee, D.-N.; Kim, H.; Mui, L.; Myung, S.-W.; Chin, J.; Kim, H.-J. Electronic Effect on the Kinetics of the Diaza-Cope Rearrangement. *J. Org. Chem.* **2009**, *74*, 3330–3334. (b) Kim, H.; Nguyen, Y.; Yen, C. P.-H.; Chagal, L.; Lough, A. J.; Kim, B. M.; Chin, J. Stereospecific Synthesis of C_2 Symmetric Diamines from the Mother Diamine by Resonance-Assisted Hydrogen-Bond Directed Diaza-Cope Rearrangement. *J. Am. Chem. Soc.* **2008**, *130*, 12184–12191. (c) Chin, J.; Mancin, F.; Thavarajah, N.; Lee, D.; Lough, A.; Chung, D. S. Controlling Diaza-Cope Rearrangement Reactions with Resonance-Assisted Hydrogen Bonds. *J. Am. Chem. Soc.* **2003**, *125*, 15276–15277.

15. Some trends seem to suggest that an –OH group in an *ortho*-position has an electron withdrawing, rather than donating effect. For example, the acidity of hydroxy-substituted benzoic acids is decreased relative to the parent benzoic acid (pK_a=4.20) when the –OH group is in the *para*-position (pK_a=4.28) but increased when the same group is *meta* (pK_a=3.84) and *ortho* (pK_a=2.98) to the –COOH functionality. See also: McDaniel, D. H.; Brown, H. C. An Extended Table of Hammett Substitutent Constants Based on the Ionization of Substituted Benzoic Acids. *J. Org. Chem.* **1958**, *23*, 420–427.

16. Jin, Y.; Yu, C.; Denman, R. Y.; Zhang, W. Recent Advances in Dynamic Covalent Chemistry. *Chem. Soc. Rev.* **2013**, *42*, 6634–6654.

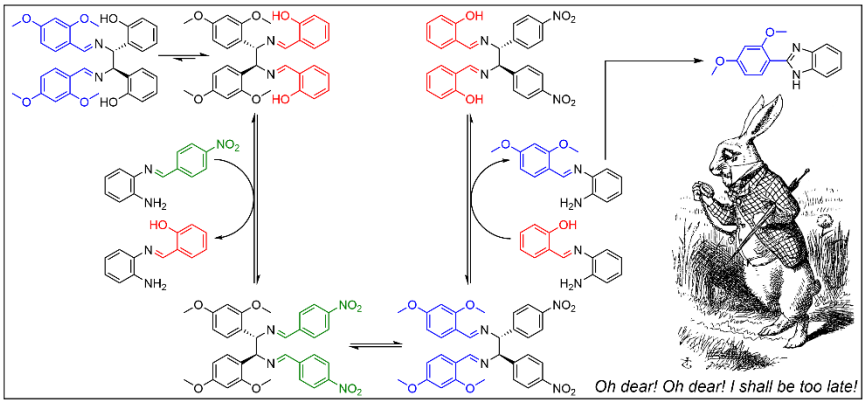
Oh dear! Oh dear! I shall be too late!

Chemoselectivity Switching through Coupled Equilibria

Thamon Puangsamlee and Ognjen Š. Miljanić*

University of Houston, Department of Chemistry, 3585 Cullen Boulevard #112, Houston, TX 77204-5003, United States
Email: miljanic@uh.edu Phone: +1.832.842.8827

Supporting Information

General Methods and Materials

All reactions were performed under nitrogen atmosphere in oven-dried glassware. Reagents were purchased from commercial suppliers and used without further purification. Solvents were used as received, except PhMe, which was dried over activated alumina in an mBraun solvent purification system.

Column chromatography was carried out on silica gel 60, 32–63 mesh. Analytical TLC was performed on J. T. Baker plastic-backed silica gel IB-F plates. *N*-(4-nitrobenzylidene)benzene-1,2-diamine was synthesized according to the literature procedure.[1] NMR spectra were obtained on JEOL ECA-500 and ECA-600 spectrometers and all ^{13}C-NMR spectra were recorded with simultaneous decoupling of ^{1}H nuclei. ^{1}H-NMR chemical shifts are reported in ppm units relative to the residual signal of the solvent ($CDCl_3$: 7.26 ppm, DMSO-d_6: 2.50 ppm). All NMR spectra were recorded at 25 °C.

Mass spectraometric measurements were performed by the Mass Spectrometry Facility of the Department of Chemistry and Biochemistry at the University of Texas at Austin. Infrared spectra were recorded on a Nicolet iS10 FT-IR spectrometer equipped with a Thermo Scientific iTR for multi-purpose ATR sampling. Melting points were measured in open capillary tubes using a Barnstead International Mel-TEMP apparatus and are uncorrected.

Experiments are presented in the order that follows the discussion of the manuscript.

Compound numbers are identical to those in the main text of the manuscript.

Synthesis of Diimine Precursors

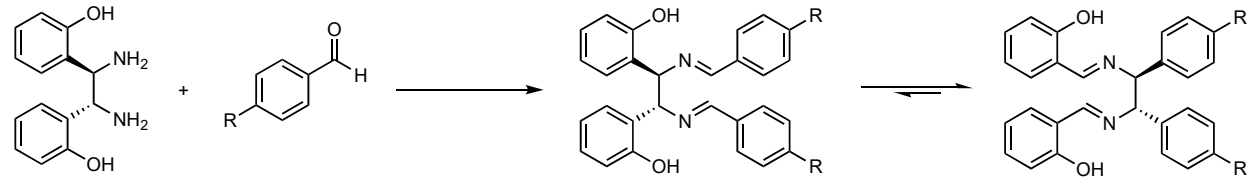

(*R*,*R*)-HPEN (**5**) **8**, **14a-e**

Procedure A: Compound (1*R*,2*R*)-1,2-bis(2-hydroxyphenyl)ethylenediamine (**5**, 500 mg, 2.05 mmol) and 2,4-dimethoxybenzaldehyde (0.71 mg, 4.27 mmol) were dissolved in DMSO (10 mL). The solution mixture was stirred overnight at room temperature. The mixture was poured into distilled H_2O (100 mL), and then the aqueous layer was extracted with Et_2O. The combined organic layers were dried over anhydrous $MgSO_4$ and then the solvent was evaporated by rotary evaporator. Crude product was purified on a silica gel column, eluting with hexane/EtOAc (3:1) + 2.5% Et_3N, to yield diimine **8** (R_f = 0.33) as a yellowish solid in 54% yield (598 mg, 1.11 mmol).

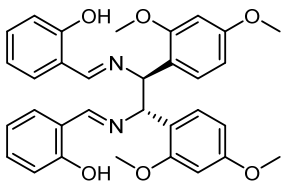

8

8: mp: 148.1–149.8 °C. ^{1}H NMR (500 MHz, DMSO-d_6): δ 13.66 (s, 2H), 8.39 (s, 2H), 7.34–7.24 (m, 4H), 7.15 (d, *J*=8.9 Hz, 2H), 6.85 (d, *J*=8.2 Hz, 2H), 6.80 (t, *J*=7.2 Hz, 2H), 6.49 (s, 2H), 6.41 (d, *J*=8.2 Hz, 2H), 5.39–5.32 (s, 2H), 3.79 (s, 6H), 3.68 (s, 6H) ppm. ^{13}C NMR (100 MHz, DMSO-d_6): δ 166.3, 161.2, 160.2, 158.1, 132.9, 132.3, 129.9, 120.7, 119.1, 105.2, 99.0, 70.6, 56.2, 55.6 ppm. IR (neat): $\tilde{\nu}$ 3002, 1623, 1610, 1499, 1278, 1259, 1208, 1158, 1132 cm^{-1}. HRMS (ESI) *m/z*: $[M+H]^+$ Calcd for $C_{32}H_{33}N_2O_6^+$: 541.2333. Found: 541.2335.

Procedure B:[2] Compound (1*R*,2*R*)-1,2-bis(2-hydroxyphenyl)ethylenediamine (**5**, 500 mg, 2.05 mmol) and an aryl aldehyde (4.92 mmol) were dissolved in MeCN (20 mL). The mixture was heated until it reached reflux and was then kept at reflux overnight. After cooling, the mixture was concentrated to one half of its original volume and left in a refrigerator overnight. The diimines precipitated as yellow solids and were collected by filtration and washed with MeCN.

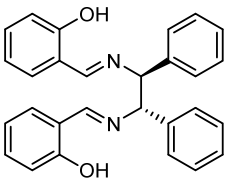

14a

14a: yellow solid (567 mg, 1.35 mmol, 66% yield). mp: 174.2–176.6 °C. ^{1}H NMR (500 MHz, DMSO-d_6): δ 13.29 (s, 2H), 8.53 (s, 2H), 7.39–7.09 (m, 14H), 6.99–6.74 (m, 4H), 5.09 (s, 2H) ppm. ^{13}C NMR (100 MHz, DMSO-d_6): δ 166.9, 160.8, 140.5, 133.1, 132.3, 128.8, 128.4, 128.0, 119.3, 119.1, 116.9, 78.2 ppm. IR (neat): $\tilde{\nu}$ 1620, 1599, 1491, 1278,1148, 1060 cm^{-1}. HRMS (ESI) *m/z*: [M+H]$^+$ Calcd for $C_{28}H_{25}N_2O_2^+$: 421.1911. Found: 421.1908.

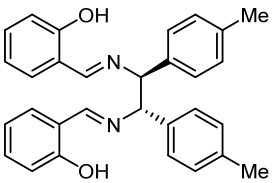

14b

14b: yellow solid (418 mg, 0.93 mmol, 45% yield). mp: 182.4–184.4 °C. ^{1}H NMR (500 MHz, DMSO-d_6): δ 13.33 (s, 2H), 8.51 (s, 2H), 7.34–7.25 (m, 4H), 7.21 (d, J = 7.6 Hz, 4H), 7.05 (d, J = 7.6 Hz, 4H), 6.90–6.77 (m, 4H), 5.03 (s, 2H), 2.19 (s, 6H) ppm. ^{13}C NMR (100 MHz, DMSO-d_6): δ 166.6, 160.8, 137.6, 136.9, 133.0, 132.3, 129.4, 128.3, 119.2, 119.1, 116.9, 77.8, 21.1 ppm. IR (neat): $\tilde{\nu}$ 1617, 1578, 1513, 1495, 1458, 1273, 1045, 1021 cm^{-1}. HRMS (ESI) *m/z*: [M+H]$^+$ Calcd for $C_{30}H_{29}N_2O_2^+$: 449.2224. Found: 449.2225.

Procedure C:[3] Compound (1*R*,2*R*)-1,2-bis(2-hydroxyphenyl)ethylenediamine (**5**, 500 mg, 2.05 mmol) and an aryl aldehyde (4.92 mmol) were dissolved in EtOH (10 mL). The mixture was stirred at room temperature to give the desired diimines as a yellow precipitate. The solid was filtered and washed with EtOH (10 mL).

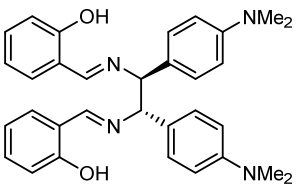

14c

14c: light yellow solid (841 mg, 1.66 mmol, 81% yield). mp: 183.3–185.7 °C. ^{1}H NMR (500 MHz, DMSO-d_6): δ 13.50 (s, 2H), 8.49 (s, 2H), 7.33–7.23 (m, 4H), 7.15 (d, J=7.6 Hz, 4H), 6.82 (q, J=7.8 Hz, 4H), 6.59 (d, J=7.6 Hz, 4H), 4.93 (s, 2H), 2.80 (s, 12H) ppm. ^{13}C NMR (100 MHz, DMSO-d_6): δ 165.8, 160.9, 150.0, 132.8, 132.1, 129.1, 128.1, 119.2, 119.1, 116.9, 112.6, 77.6, 40.5 ppm. IR (neat): $\tilde{\nu}$ 1624, 1613, 1577, 1522, 1459, 1443, 1354, 1274, 1166, 1151 cm^{-1}. HRMS (ESI) *m/z*: [M+H]$^+$ Calcd for $C_{32}H_{35}N_4O_2^+$: 507.2755. Found: 507.2760.

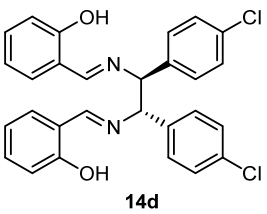

14d

14d: yellow solid (889 mg, 1.82 mmol, 89% yield). mp: 199.1–201.4 °C. ^{1}H NMR (500 MHz, DMSO-d_6): δ 13.08 (s, 2H), 8.54 (s, 2H), 7.37–7.27 (m, 12H), 6.98–6.70 (m, 4H), 5.11 (s, 2H) ppm. ^{13}C NMR (100 MHz, DMSO-d_6): δ 167.3, 160.7, 139.3, 133.3, 132.6, 132.3, 130.3, 128.9, 119.4, 119.0, 117.0, 77.2 ppm. IR (neat): $\tilde{\nu}$ 1622, 1578, 1489, 1275, 1012, 824, 755, 733 cm^{-1}. HRMS (ESI) *m/z*: $[M+H]^+$ Calcd for $C_{28}H_{23}Cl_2N_2O_2^+$: 489.1131. Found: 489.1129.

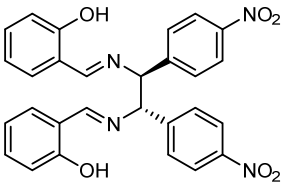

14e

14e: yellow solid (781 mg, 1.53 mmol, 75% yield). mp: 206.0–208.1 °C. ^{1}H NMR (500 MHz, DMSO-d_6: δ 12.79 (s, 2H), 8.57 (s, 2H), 8.12 (d, *J*=8.2 Hz, 4H), 7.60 (d, *J*=8.2 Hz, 4H), 7.34 (d, *J*=7.6 Hz, 2H), 7.28 (t, *J*=7.9 Hz, 2H), 6.93–6.75 (m, 4H), 5.34 (s, 2H) ppm. ^{13}C NMR (100 MHz, DMSO-d_6): δ 168.0, 160.5, 147.6, 147.4, 133.5, 132.4, 129.8, 124.1, 119.5, 119.1, 117.0, 76.9 ppm. IR (neat): $\tilde{\nu}$ 1626, 1696, 1531, 1519, 1489, 1348, 1275, 856, 754 cm^{-1}. HRMS (ESI) *m/z*: $[M+H]^+$ Calcd for $C_{28}H_{23}N_4O_6^+$: 511.1612. Found: 511.1612.

Oxidation of a Mixture of Diimine 8 and Diamine 3

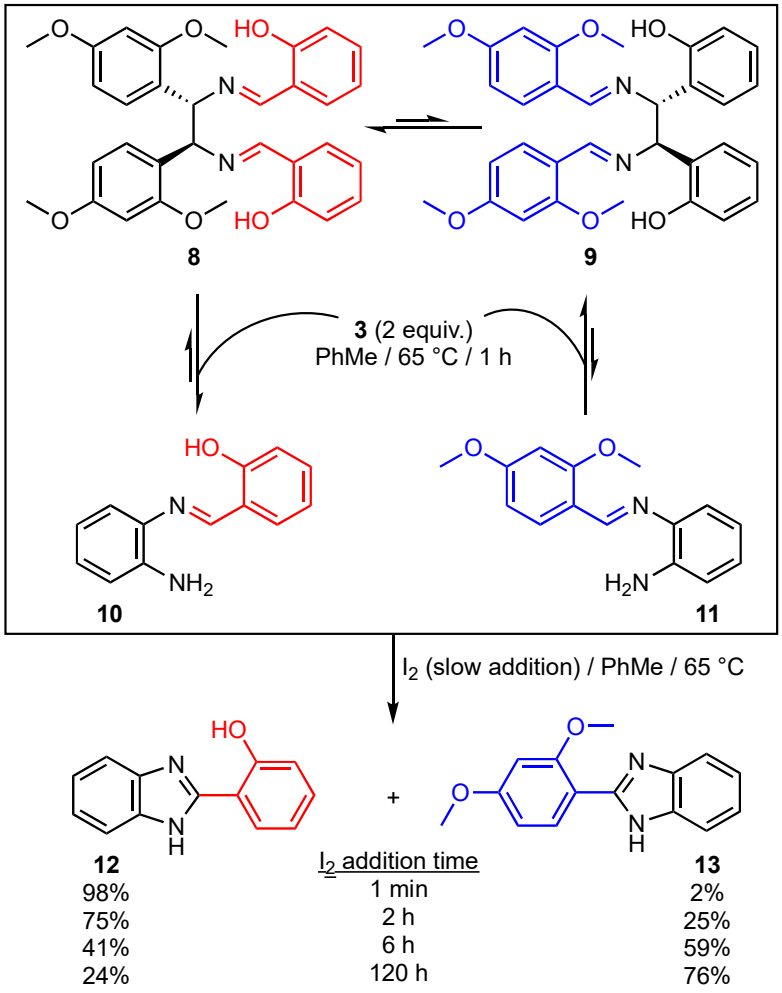

Diimine **8** (100 mg, 0.18 mmol) and 1,2-phenylenediamine (**3**, 38.9 mg, 0.36 mmol) were dissolved in PhMe (7 mL) and heated at 65 °C for 1 h. Solution of I_2 (91.3 mg, 0.36 mmol) in PhMe (24 mL) was injected via a syringe pump at several different rates. After I_2 was added, the solution mixture was heated at 65 °C for 24 h. A brown precipitate formed during addition. After 24 h, the mixture was washed with a saturated aqueous solution of $Na_2S_2O_3$ and then extracted with EtOAc. The organic layer was collected and dried over $MgSO_4$. The crude product was analyzed by ^{1}H NMR spectroscopy in DMSO-d_6 to calculate the yields of products by using 1,3,5-trimethoxybenzene as the internal standard.[4]

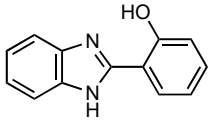

12

2-(2-hydroxyphenyl)benzimidazole (**12**): ^{1}H NMR (500 MHz, DMSO-d_6): δ 11.95 (s, 1H), 8.28 (d, J=8.6 Hz, 1H), 7.60 (s, 2H), 7.16 (s, 2H), 6.85–6.62 (m, 2H), 4.02 (s, 3H), 3.86 (s, 3H) ppm. ^{13}C NMR (100 MHz, DMSO-d_6): δ 162.5, 158.6, 149.8,

143.4, 135.2, 131.4, 122.1, 121.8, 118.6, 112.2, 111.7, 106.8, 99.1, 56.4, 56.0 ppm. This data agrees with a previous literature report.[6]

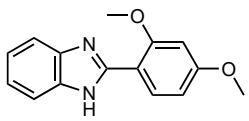

13

2-(2,4-dimethoxyphenyl)benzimidazole (**13**): ^{1}H NMR (500 MHz, DMSO-d_6): δ 13.18 (s, 2H), 8.06 (d, J=8.0 Hz, 1H), 7.67 (s, 2H), 7.38 (t, J=7.7 Hz, 1H), 7.28 (s, 2H), 7.03 (q, J=8.2 Hz, 2H) ppm. ^{13}C NMR (100 MHz, DMSO-d_6): δ 155.3, 149.0, 138.0, 129.0, 123.5, 120.0, 116.4, 115.1, 114.5, 109.9 ppm. This data agrees with a previous literature report.[5]

Relative ration of product **12** and **13** varied with temperature and the rate of addition of I_2. If I_2 was added over 1 min, **12** was favored by 98:2 at 65 °C and 89:11 at 90 °C. Addition of I_2 over 120 h caused this ratio to switch to favor **13**: 24:76 at 65 °C and 9:91 at 90 °C.

Chemoselectivity Switching with Different Diimine Starting Materials

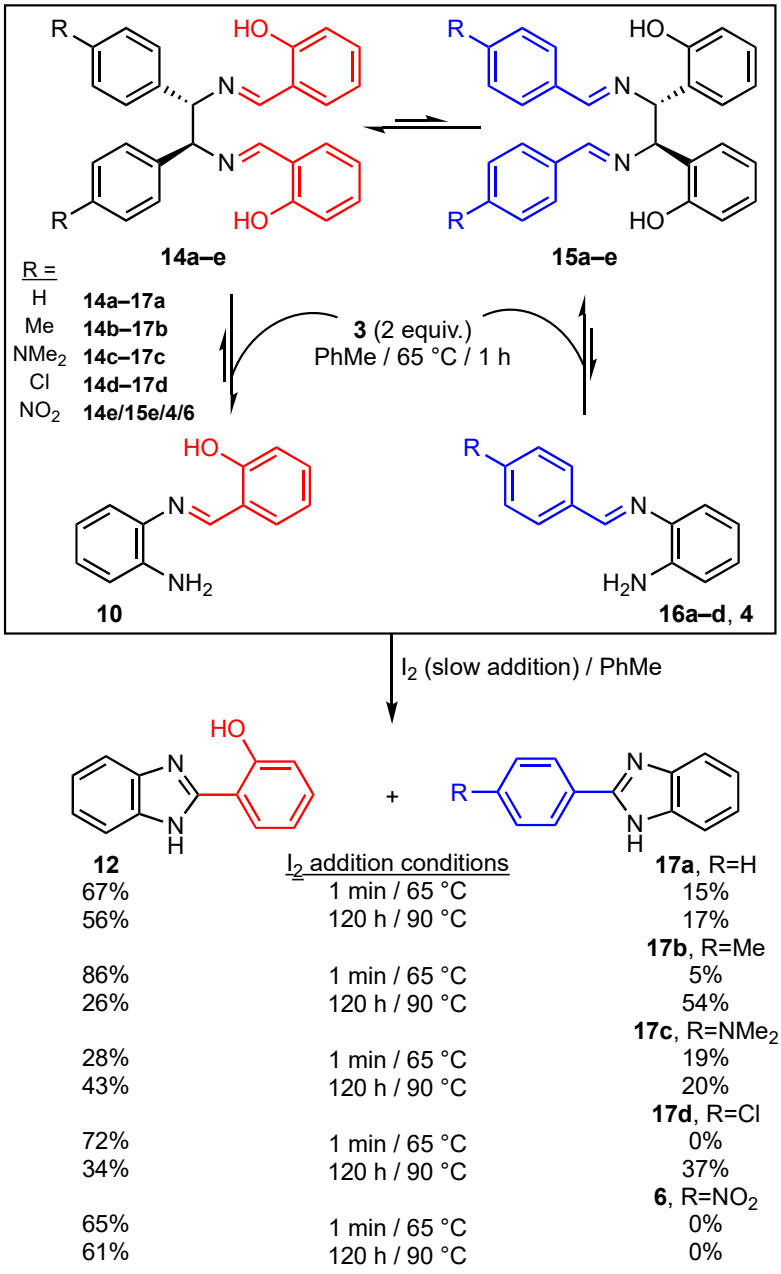

Fast Addition of I_2. Diimine of choice (0.18 mmol) and 1,2-phenylenediamine (**3**, 38.9 mg, 0.36 mmol) were dissolved in PhMe (7 mL) and heated up to 65 °C. Solution of I_2 (91.3 mg, 0.36 mmol) in PhMe (24 mL) was quickly injected into the reaction mixture within 1 min and the reaction mixture was stirred at 65 °C for 24 h. After that time, the mixture was washed with a saturated aqueous solution of $Na_2S_2O_3$ and then extracted with EtOAc. The organic layer was collected and dried over anhydrous

$MgSO_4$. The solvent was then removed and the brown solid residue was analyzed by ^1H NMR spectroscopy to determine the yield of respective products via the internal standard method. The crude products were purified on a silica gel column, eluting with a 7:3 hexane/EtOAc mixture.

Oxidation of diimine **8**: Product 2-(2-hydroxyphenyl)benzimidazole (**12**, R_f = 0.5) was first obtained as a white solid in 51% yield (38.6 mg, 0.18 mmol) from column chromatography eluting with a 7:3 hexane/EtOAc mixture. Then, chromatography column was eluted with a 3:2 hexane/Me_2CO mixture to afford 2-(2,4-dimethoxyphenyl)benzimidazole (**13**, R_f = 0.2) as a pale brown solid in 2% yield (1.8 mg, 0.01 mmol).

Oxidation of diimine **14a**: After column chromatography eluting with a 7:3 hexane/EtOAc mixture, product 2-(2-hydroxyphenyl)benzimidazole (**12**, R_f = 0.5) was first obtained as a white solid in 67% yield (51.0 mg, 0.24 mmol). Then, 2-phenylbenzimidazole (**17a**, R_f = 0.2) was collected as a white solid in 15% yield (12.8 mg, 0.05 mmol).

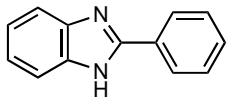

17a

17a: ^1H NMR (500 MHz, DMSO-d_6): δ 8.20 (d, J=7.6 Hz, 2H), 7.62 (t, J=3.1 Hz, 2H), 7.56 (t, J=7.2 Hz, 2H), 7.53–7.46 (1H), 7.22 (t, J=3.1 Hz, 2H) ppm. ^{13}C NMR (DMSO-d_6, 100 MHz): δ 151.7, 139.8, 130.6, 130.4, 129.5, 127.0, 122.7, 115.6 ppm. This data agrees with a previous literature report.[6]

Oxidation of diimine **14b**: After column chromatography eluting with a 7:3 hexane/EtOAc mixture, 2-(2-hydroxyphenyl)benzimidazole (**12**, R_f = 0.5) was first obtained as a white solid in 86% yield (65.0 mg, 0.31 mmol). In the second fraction, 2-(4-methylphenyl)benzimidazole (**17b**, R_f = 0.2) was collected as a white solid in 5% yield (3.7 mg, 0.02 mmol).

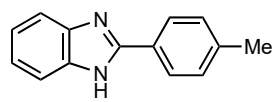

17b

17b: ^1H NMR (500 MHz, DMSO-d_6): δ 8.09 (d, J = 7.6 Hz, 2H), 7.59 (t, J = 3.1 Hz, 2H), 7.35 (d, J=7.6 Hz, 2H), 7.19 (t, J=3.1 Hz, 2H), 2.37 (s, 3H) ppm. ^{13}C NMR (100 MHz, DMSO-d_6): δ 152.0, 140.0, 130.0, 128.1, 127.0, 122.4 ppm. This data agrees with a previous literature report.[5]

Oxidation of diimine **14c**: After column chromatography eluting with a 7:3 hexane/EtOAc mixture, 2-(2-hydroxyphenyl)benzimidazole (**12**, R_f = 0.5) was first obtained as a white solid in 28% yield (21.2 mg, 0.10 mmol). In the second fraction, 2-(4-dimethylaminophenyl)benzimidazole (**17c**, R_f = 0.1) was collected as a white solid in 19% yield (16.2 mg, 0.07 mmol).

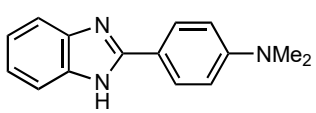

17c

17c: ^{1}H NMR (500 MHz, DMSO-d_6): δ 8.00 (d, J=7.6 Hz, 2H), 7.50 (d, J=2.1 Hz, 2H), 7.12 (t, J=3.1 Hz, 2H), 6.83 (d, J=7.6 Hz, 2H), 2.98 (d, J=10.3 Hz, 6H) ppm. ^{13}C NMR (100 MHz, DMSO-d_6): δ 152.8, 151.8, 128.1, 121.8, 118.0, 112.4, 40.4 ppm. This data agrees with a previous literature report.[7]

Oxidation of diimine **14d**: Only 2-(2-hydroxyphenyl)benzimidazole (**12**, R_f = 0.4) was eluted as a white solid in 72% yield (54.5 mg, 0.26 mmol) from column chromatography where a 7:3 hexane/EtOAc mixture was used as the eluent.

Oxidation of diimine **14e**: Only 2-(2-hydroxyphenyl)benzimidazole (**12**, R_f = 0.5) was obtained as a white solid in 65% yield (49.2 mg, 0.23 mmol) from column chromatography where a 7:3 hexane/EtOAc mixture was used as the eluent.

Slow Addition of I_2. Diimine of choice (0.18 mmol) and 1,2-phenylenediamine (**3**, 38.9 mg, 0.36 mmol) were dissolved in PhMe (7 mL) and heated up to 90 °C. A solution of I_2 (91.3 mg, 0.36 mmol) in PhMe (120 mL) was slowly injected into the reaction mixture using a syringe pump (rate 1 mL/h) and the solution was stirred at 90 °C for 1 h. After that time, the mixture was washed with a saturated aqueous solution of $Na_2S_2O_3$ and extracted with EtOAc. The organic layer was collected and dried over anhydrous $MgSO_4$. Solvent was then removed and the brown solid residue was analyzed by ^{1}H NMR spectroscopy to calculate the yields. The crude products were purified on a silica gel column, eluting with a 7:3 hexane/EtOAc mixture.

Oxidation of diimine **8**: 2-(2-hydroxyphenyl)benzimidazole (**12**, R_f = 0.5) was first obtained as a white solid in 5% yield (3.8 mg, 0.02 mmol) from column chromatography eluting with a 7:3 hexane/EtOAc mixture. The second fraction was eluted using a 3:2 hexane/Me_2CO mixture to afford 2-(2,4-dimethoxyphenyl)benzimidazole (**13**, R_f = 0.2) as a pale brown solid in 44% yield (40.3 mg, 0.16 mmol).

Oxidation of diimine **14a**: After column chromatography eluting with a 7:3 hexane/EtOAc mixture, 2-(2-hydroxyphenyl)benzimidazole (**12**, R_f = 0.5) was first obtained as a white solid in 56% yield (42.4 mg, 0.20 mmol). In the second fraction, 2-phenylbenzimidazole (**17a**, R_f = 0.2) was collected as a white solid in 17% yield (11.9 mg, 0.06 mmol).

Oxidation of diimine **14b**: After column chromatography eluting with a 7:3 hexane/EtOAc mixture, 2-(2-hydroxyphenyl)benzimidazole (**12**, R_f = 0.5) was first obtained as a white solid in 26% yield (19.7 mg, 0.09 mmol). In the second fraction, 2-(4-methylphenyl)benzimidazole (**17b**, R_f = 0.2) was collected as a white solid in 54% yield (40.5 mg, 0.19 mmol).

Oxidation of diimine **14c**: After column chromatography eluting with a 7:3 hexane/EtOAc mixture, 2-(2-hydroxyphenyl)benzimidazole (**12**, R_f = 0.5) was first obtained as a white solid in 43% yield (32.5 mg, 0.15 mmol). In the second fraction, 2-(4-dimethylaminophenyl)benzimidazole (**17c**, R_f = 0.1) was collected as a white solid in 20% yield (17.1 mg, 0.07 mmol).

Oxidation of diimine **14d**: After column chromatography eluting with a 7:3 hexane/EtOAc mixture, 2-(2-hydroxyphenyl)benzimidazole (**12**, R_f = 0.5) was first obtained as a white solid in 34% yield (25.7 mg, 0.12 mmol). In the second fraction, 2-(4-chlorophenyl)benzimidazole (**17d**, R_f = 0.4) was eluted as a white solid in 37% yield (30.5 mg, 0.13 mmol).

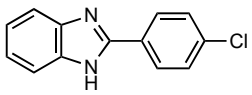

17d

17d: ^{1}H NMR (500 MHz, DMSO-d_6): δ 12.97 (s, 1H), 8.19 (d, J = 8.2 Hz, 2H), 7.62 (d, J = 8.2 Hz, 4H), 7.22 (q, J = 2.5 Hz, 2H) ppm. ^{13}C NMR (100 MHz, DMSO-d_6): δ 150.7, 135.0, 129.6, 128.7, 122.8 ppm. This data agrees with a previous literature report.[6]

Oxidation of diimine **14e**: Only 2-(2-hydroxyphenyl)benzimidazole (**12**, R_f = 0.5) was obtained as a white solid in 61% yield (46.2 mg, 0.22 mmol) from column chromatography which used a 7:3 hexane/EtOAc mixture as the eluent.

Chemoselectivity Switching between Three Possible Products

To perform these experiments, diimine **8** (100 mg, 0.18 mmol) and *N*-(4-nitrobenzylidene) benzene-1,2-diamine (**4**, 86.9 mg, 0.36 mmol) were dissolved in PhMe (7 mL) and stirred at 65 °C for 1 h. Then, 2 eq. of I_2 (91.3 mg, 0.36 mmol) were dissolved in PhMe (24 mL) and added to reaction mixture using a syringe pump at several different addition rate, as shown in the Table below. After the addition of I_2, the mixture was stirred at 65 °C for 24 h. Then, the solvent was removed under vacuum. Product ratios were determined based on the integration of ^{1}H NMR spectra of the crude products from the reactions. Spectra were recorded in DMSO-d_6 using 1,3,5-trimethoxybenzene as an internal standard. Ratios in the Table are the relative ^{1}H NMR yields of benzimidazoles **12**, **13**, and **6**.

Table 2. Relative of three benzimidazole products

Addition time	Rate of addition	Ratio of three-products		
		12	**13**	**6**
1 minute	24 mL/min	3	1	96
1 h	24 mL/h	54	46	0
2 h	12 mL/h	68	32	0
3 h 3h	8 mL/h	59	41	0
4 h	6 mL/h	65	35	0
5 h	4.8 mL/h	39	61	0
6 h	4 mL/h	38	62	0
24 h	1 mL/h	39	61	0
120 h*	1 mL/h	77	93	0

*Iodine was dissolved in PhMe (120 mL), the mixture was left at 65 °C for 1 h after

For comparison, pure samples of all relevant benzimidazoles were prepared by mixing equimolar amounts of 1,2-phenylenediamine (**3**) and corresponding aldehydes in PhMe at 65 °C and then oxidizing the obtained imine with 1 eq. of iodine

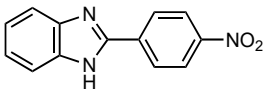

6

2-(4-nitrophenyl)benzimidazole (**6**): ^{1}H NMR (500 MHz, DMSO-d_6): δ 8.55 (d, J = 8.5 Hz, 2H), 8.41 (d, J = 8.5 Hz, 2H), 7.86–7.85 (m, 2H), 7.57–7.55 (m, 2H) ppm. ^{13}C NMR (100 MHz, DMSO-d_6): δ 149.9, 147.9, 134.2, 129.6, 126.4, 125.2, 121.0, 115.2 ppm. This data agrees with a previous literature report.[6]

^{1}H and ^{13}C NMR Spectra of Diimine Precursors

Figure 1. ^{1}H NMR Spectrum of compound **8**.

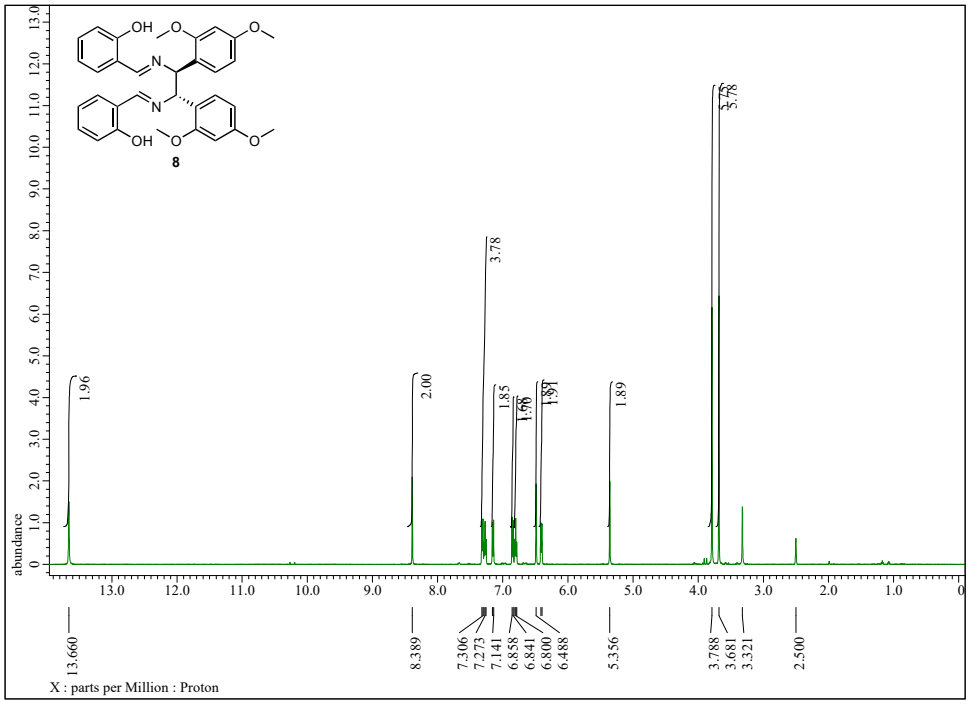

Figure 2. ^{13}C NMR Spectrum of compound **8**.

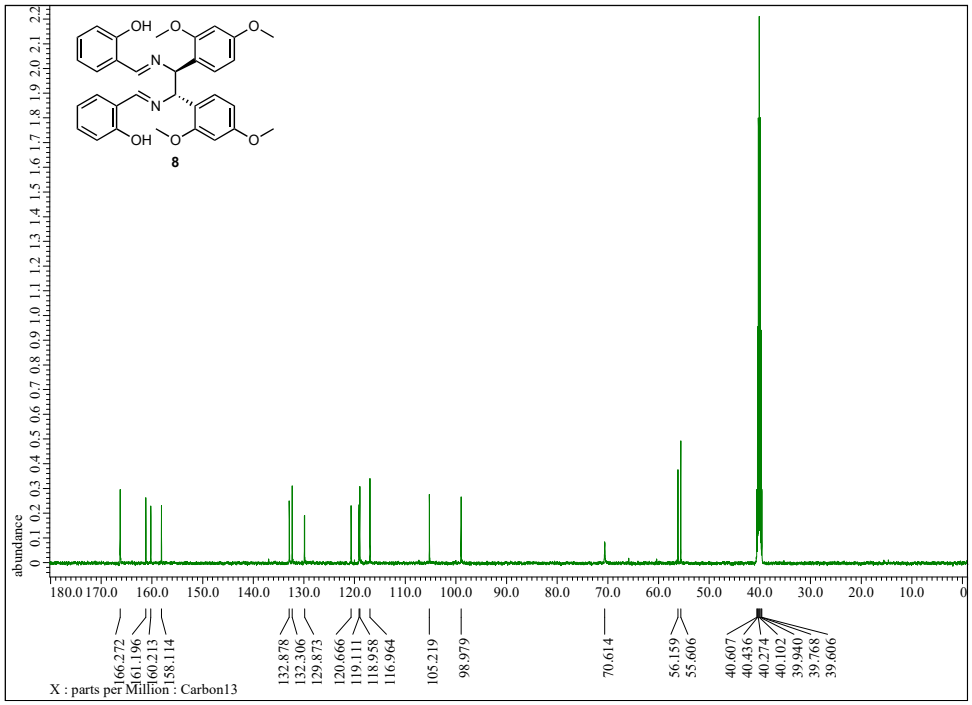

Figure 3. [1]H NMR Spectrum of compound **14a**.

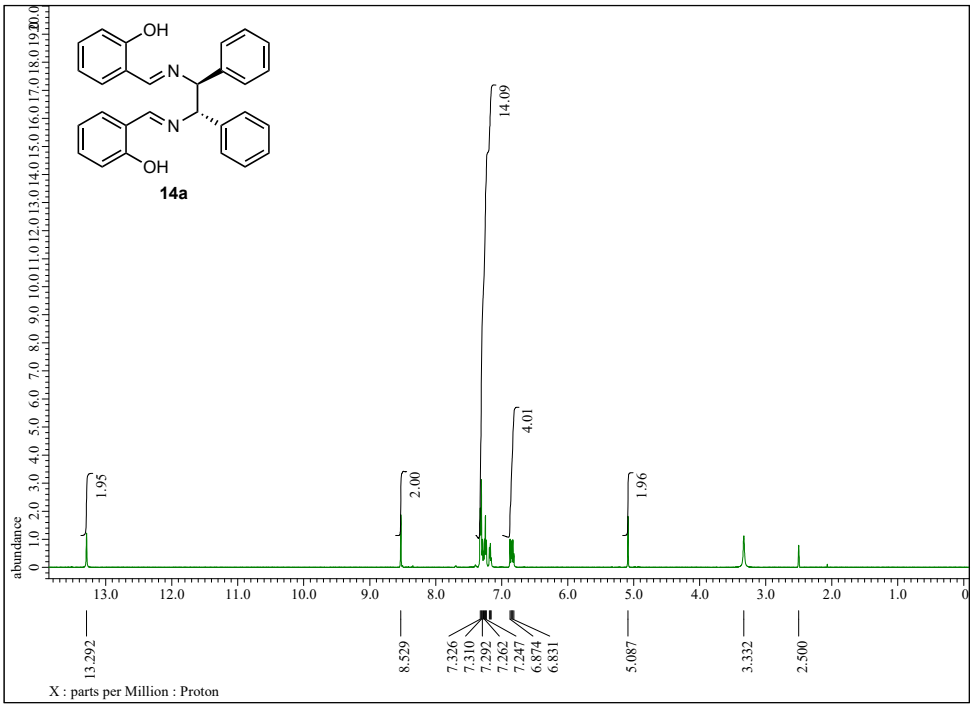

Figure 4. [13]C NMR Spectrum of compound **14a**.

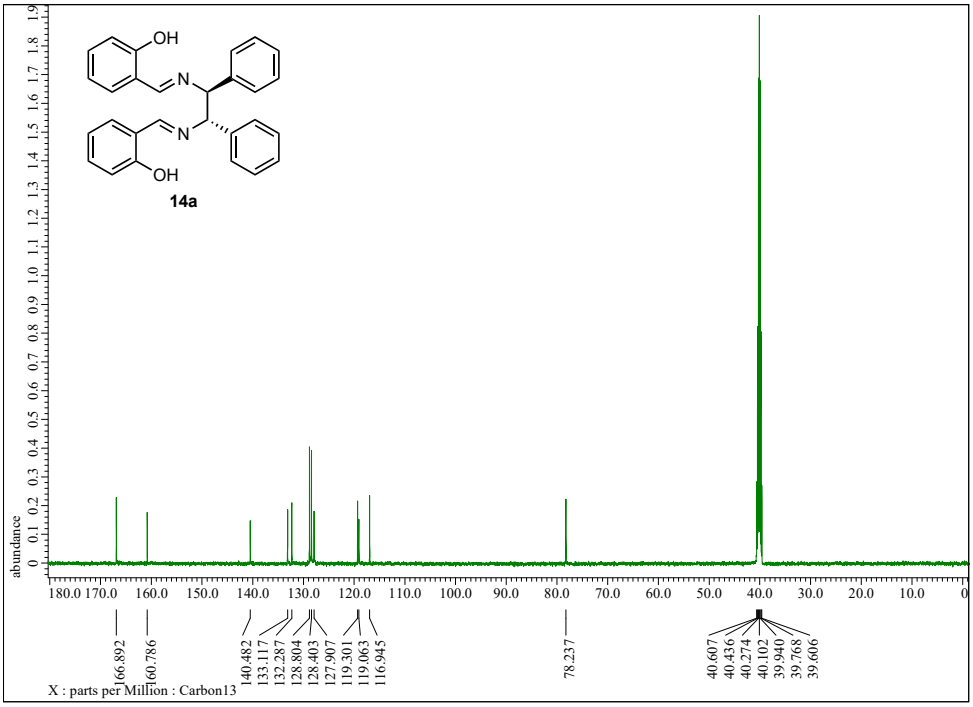

Figure 5. ^{1}H NMR Spectrum of compound **14b**.

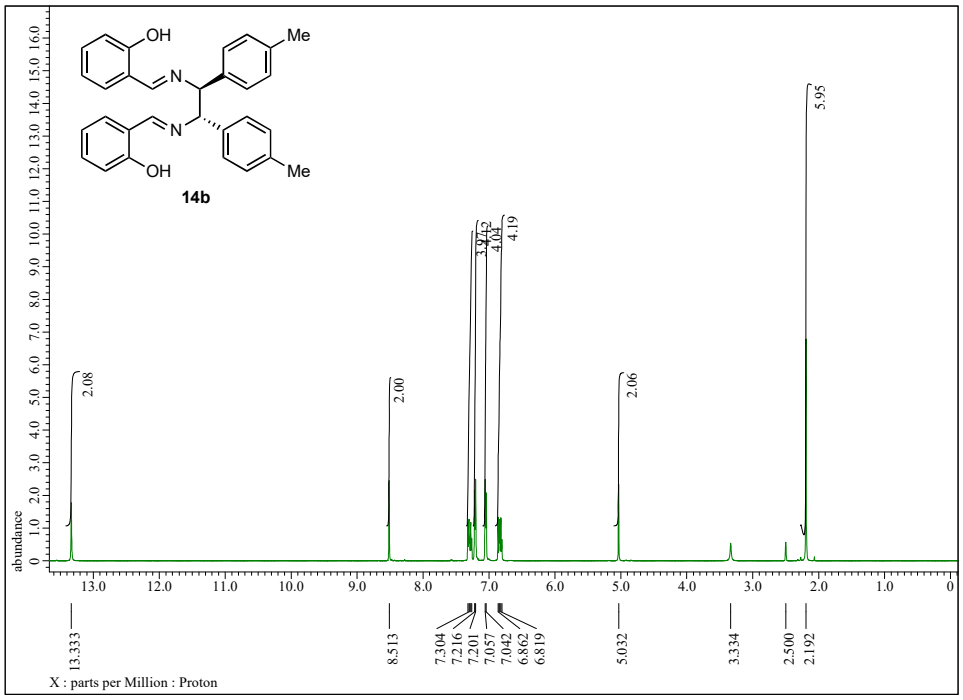

Figure 6. ^{13}C NMR Spectrum of compound **14b**.

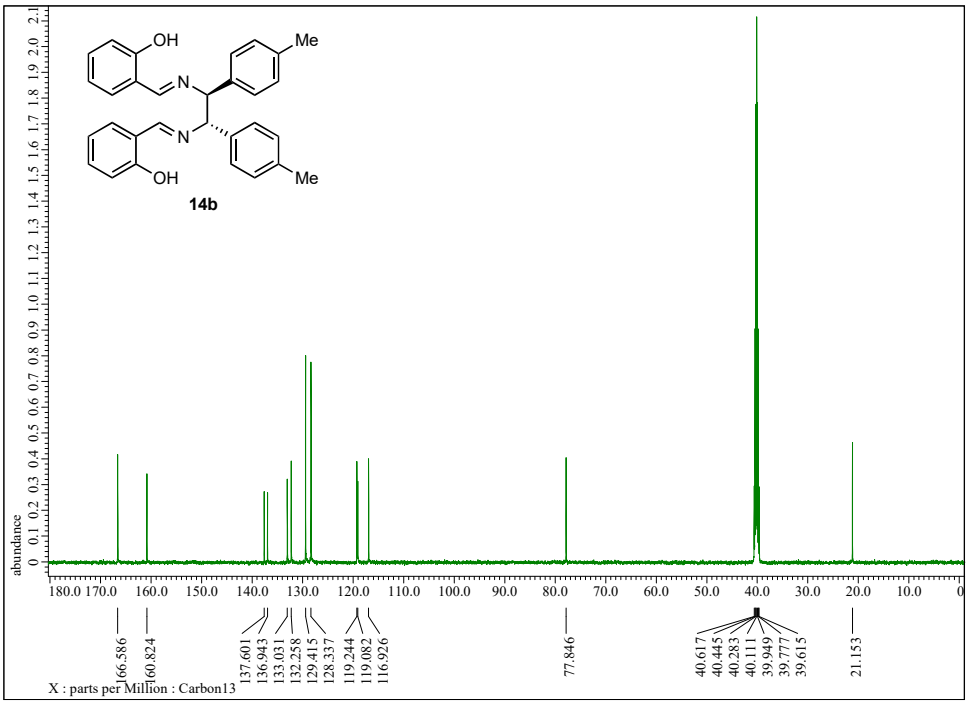

Figure 7. ^{1}H NMR Spectrum of compound **14c**.

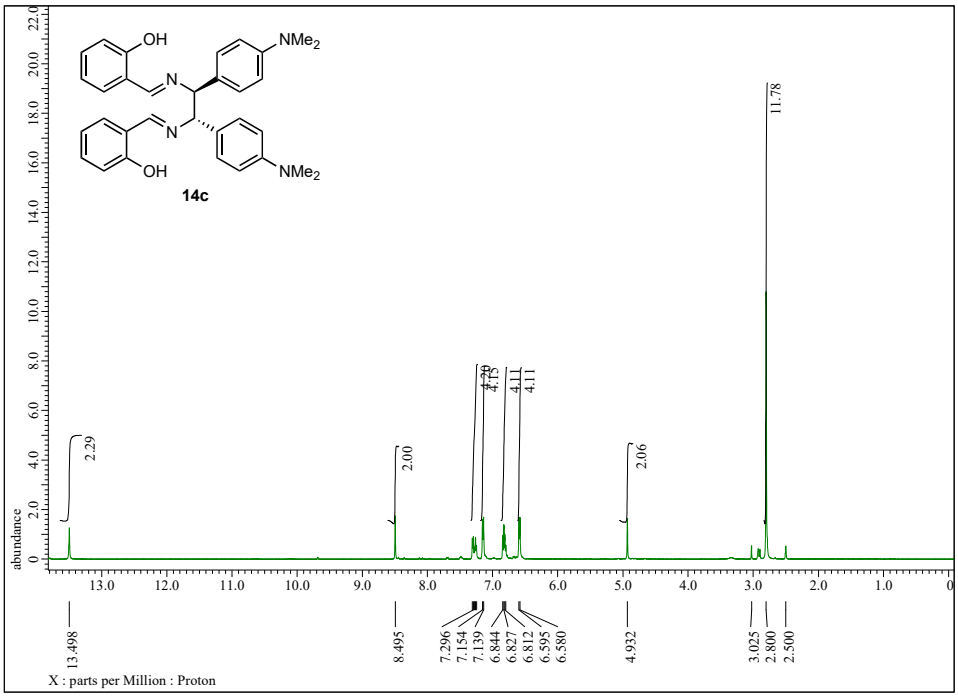

Figure 8. ^{13}C NMR Spectrum of compound **14c**.

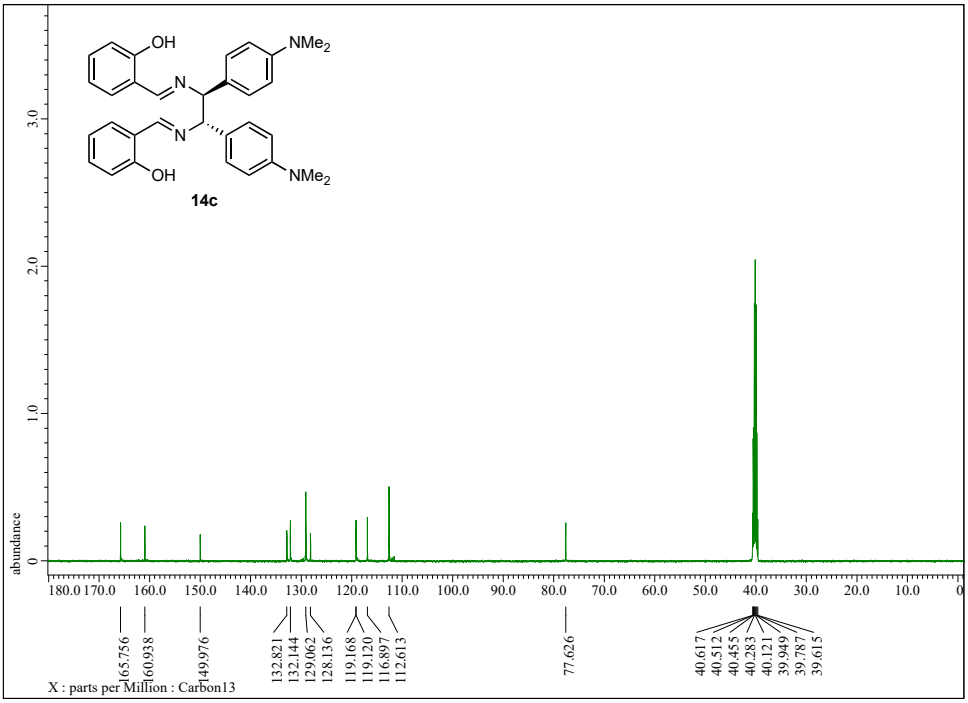

Figure 9. [1]H NMR Spectrum of compound **14d**.

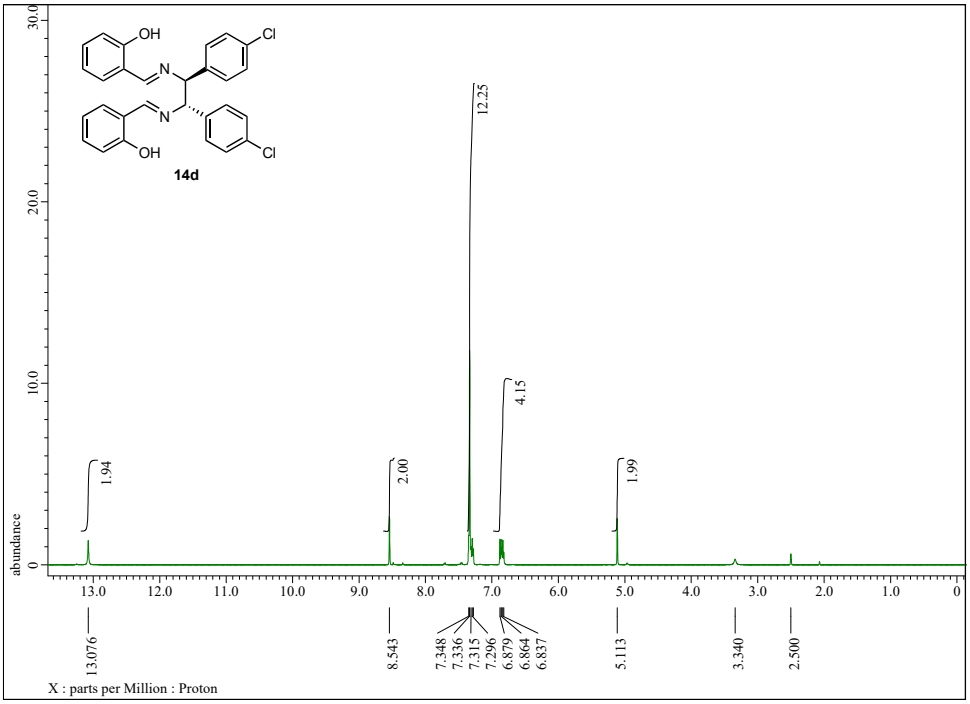

Figure 10. [13]C NMR Spectrum of spectrum **14d**.

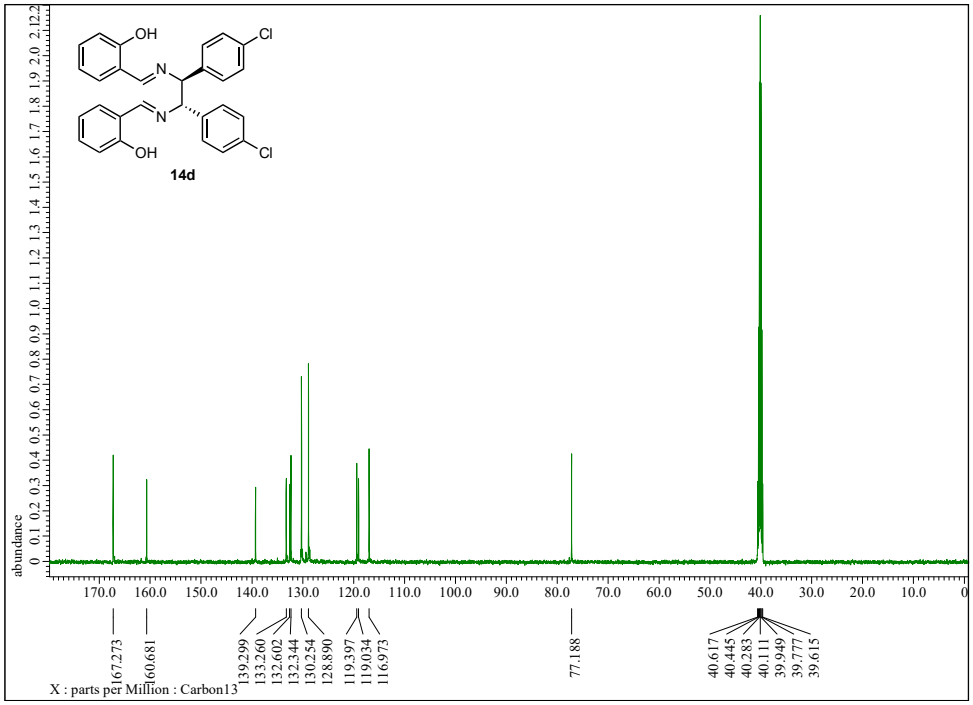

Figure 11. ^{1}H NMR Spectrum of compound **14e**.

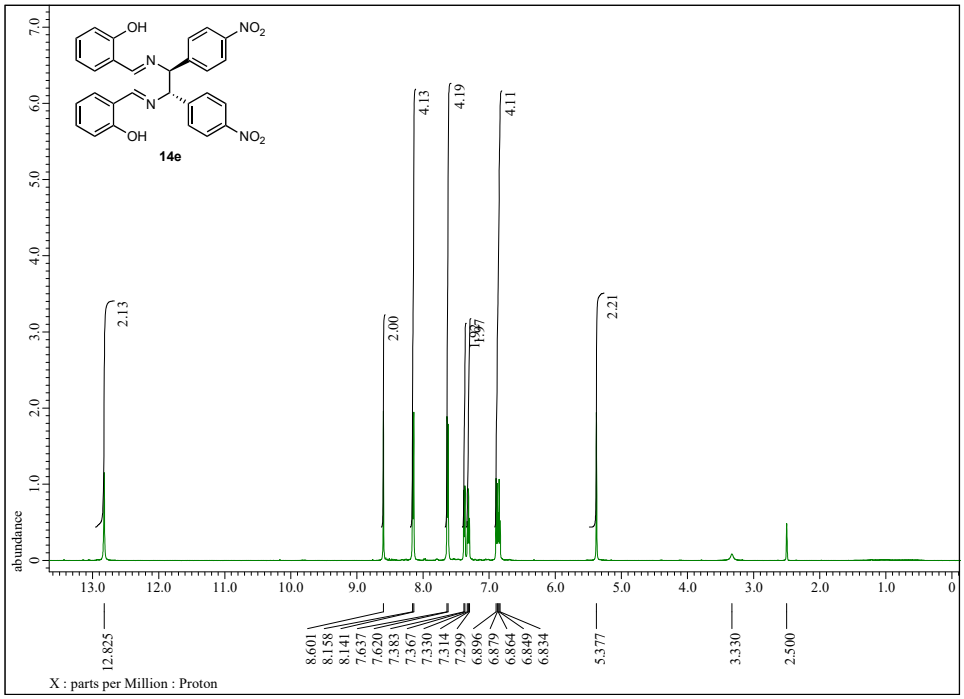

Figure 12. ^{13}C NMR Spectrum of compound **14e**.

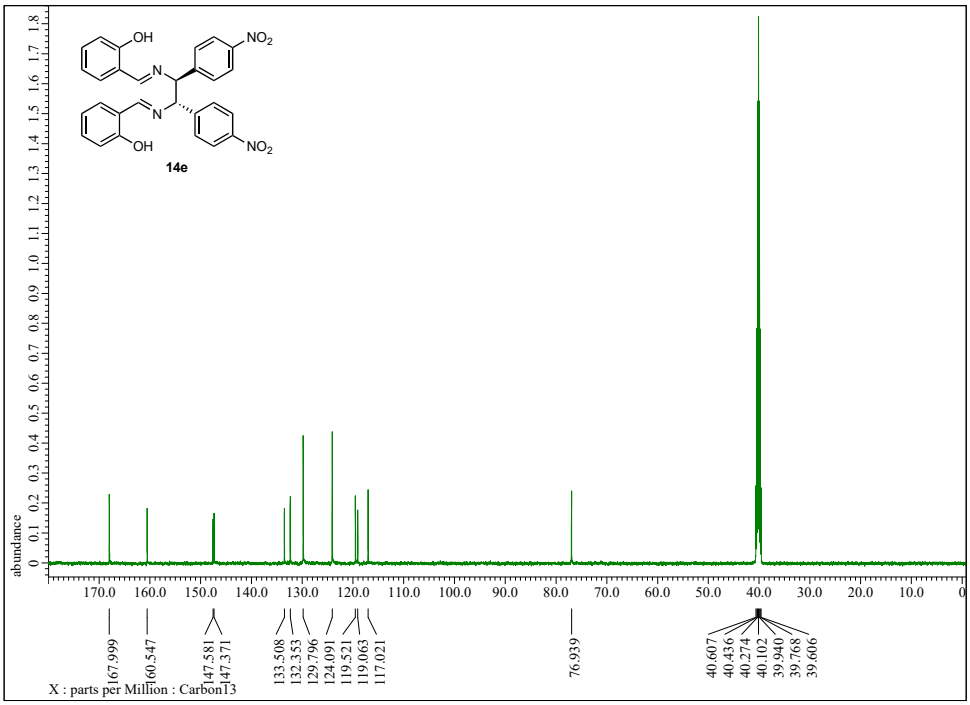

[1]H NMR Spectra of Product Mixtures Obtained after Fast Oxidations

Figure 13. [1]H NMR Spectrum of the product mixture obtained by fast oxidation of a mixture of diimine **8** and **3**. Critical peaks belonging to **12** are marked with a ● and those belonging to **13** with a ■.

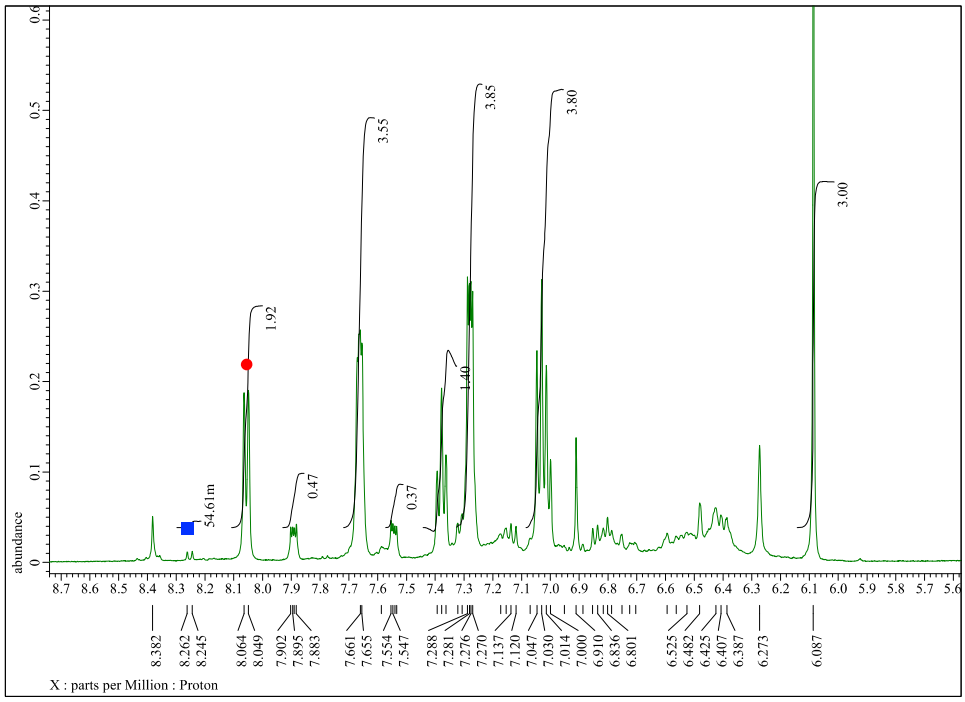

Figure 14. [1]H NMR Spectrum of the product mixture obtained by fast oxidation of a mixture of diimine **14a** and **3**. Critical peaks belonging to **12** are marked with a ● and those belonging to **17a** with a ■.

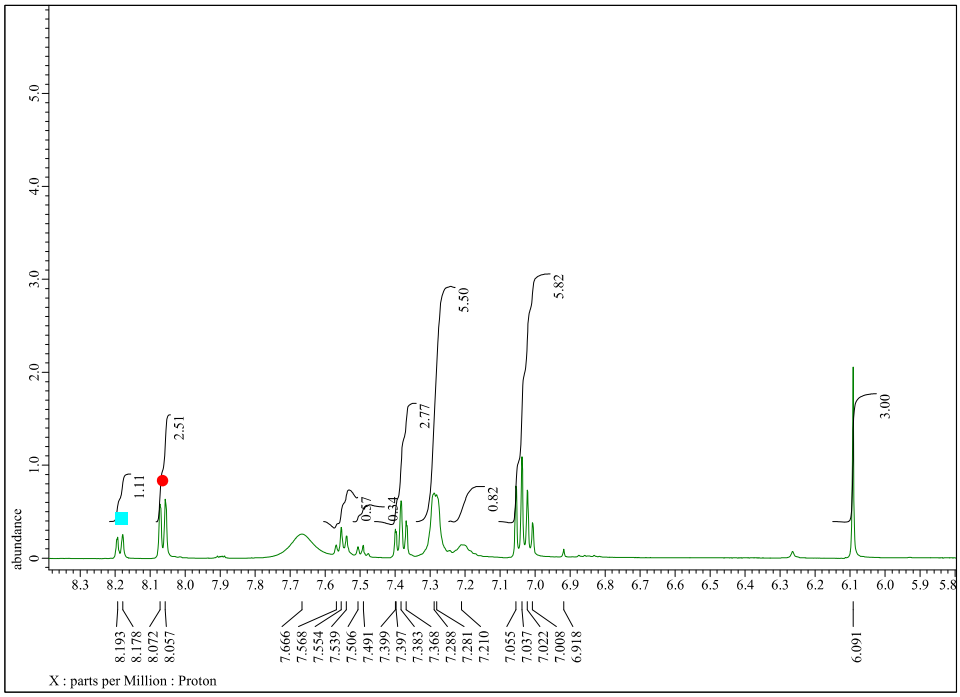

Figure 15. ^{1}H NMR Spectrum of the product mixture obtained by fast oxidation of a mixture of diimine **14b** and **3**. Critical peaks belonging to **12** are marked with a ● and those belonging to **17b** with a ■.

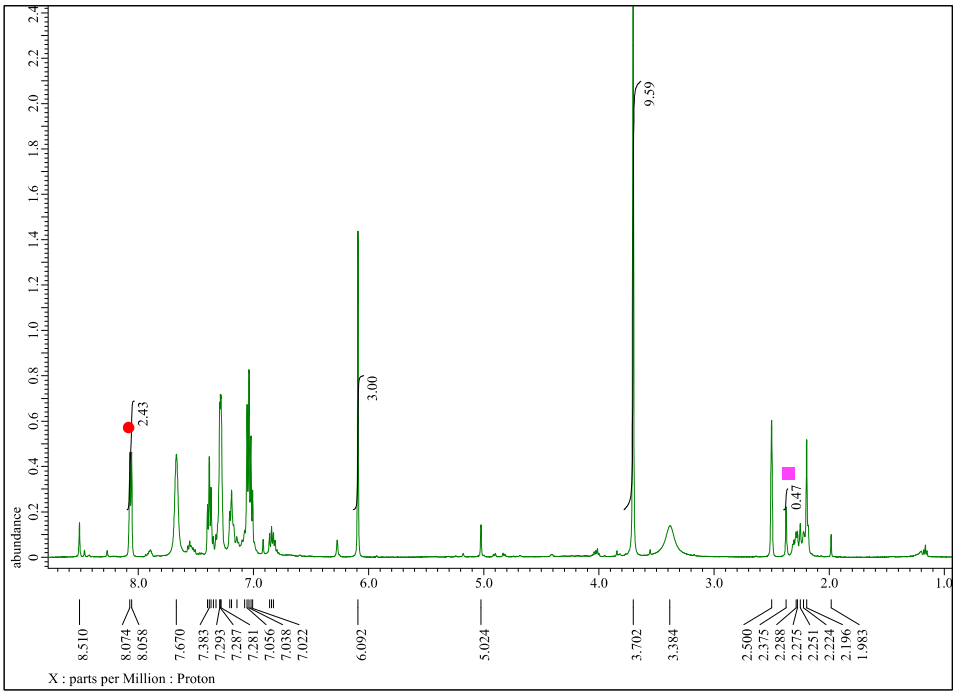

Figure 16. ^{1}H NMR Spectrum of the product mixture obtained by fast oxidation of a mixture of diimine **14c** and **3**. Critical peaks belonging to **12** are marked with a ● and those belonging to **17c** with a ■.

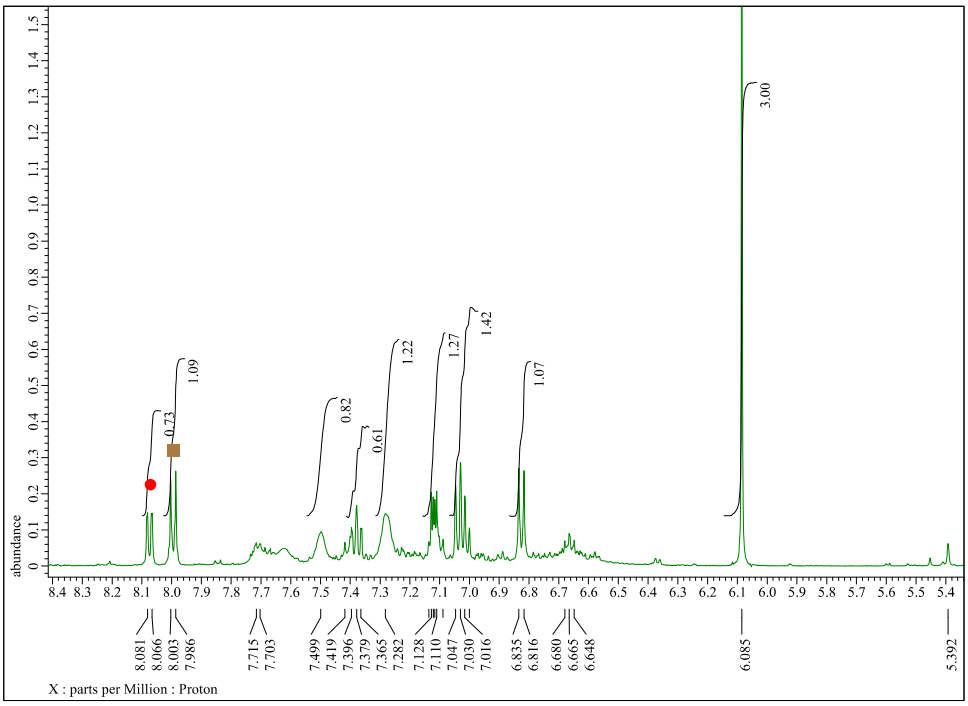

Figure 17. [1]H NMR Spectrum of the product mixture obtained by fast oxidation of a mixture of diimine **14d** and **3**. Critical peaks belonging to **12** are marked with a ● and those belonging to **17d** with a ■.

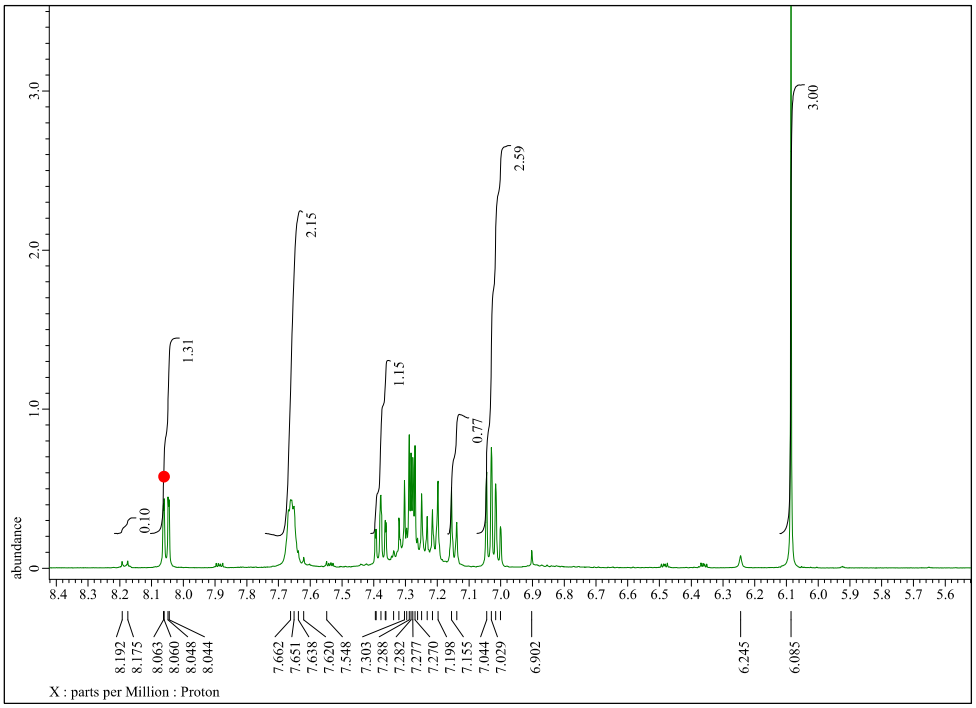

Figure 18. [1]H NMR Spectrum of the product mixture obtained by fast oxidation of a mixture of diimine **14e** and **3**. Critical peaks belonging to **12** are marked with a ● and those belonging to **6** with a ▲.

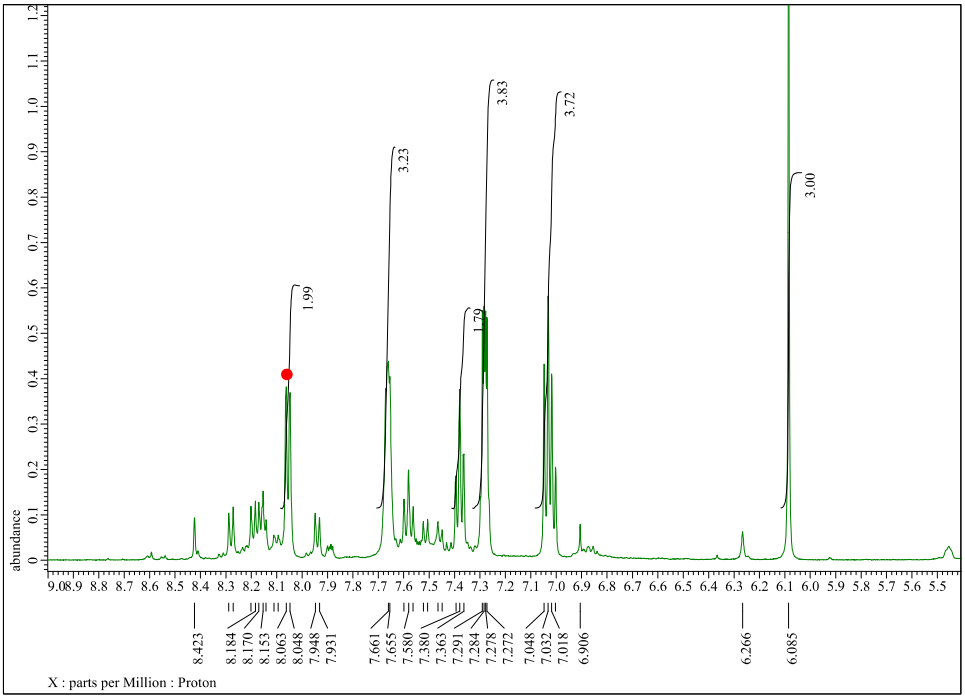

^{1}H NMR Spectra of Product Mixtures Obtained after Slow Oxidations

Figure 19. ^{1}H NMR Spectrum of the product mixture obtained by slow oxidation of a mixture of diimine **8** and **3**. Critical peaks belonging to **12** are marked with a ● and those belonging to **13** with a ■.

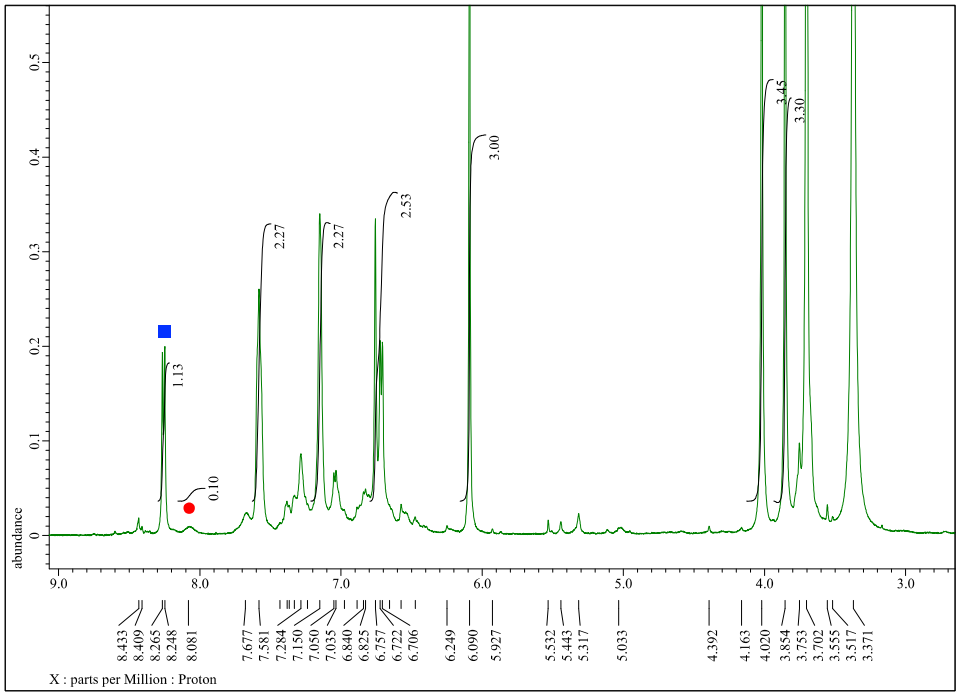

Figure 20. ^{1}H NMR Spectrum of the product mixture obtained by slow oxidation of a mixture of diimine **14a** and **3**. Critical peaks belonging to **12** are marked with a ● and those belonging to **17a** with a ■.

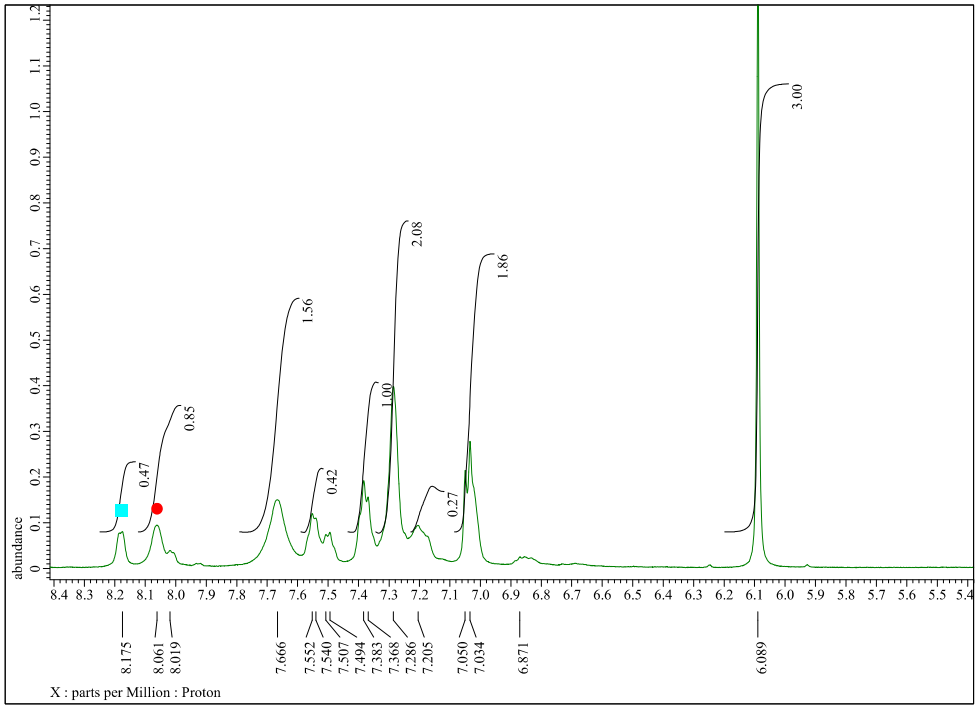

Figure 21. ^{1}H NMR Spectrum of the product mixture obtained by slow oxidation of a mixture of diimine **14b** and **3**. Critical peaks belonging to **12** are marked with a ● and those belonging to **17b** with a ■.

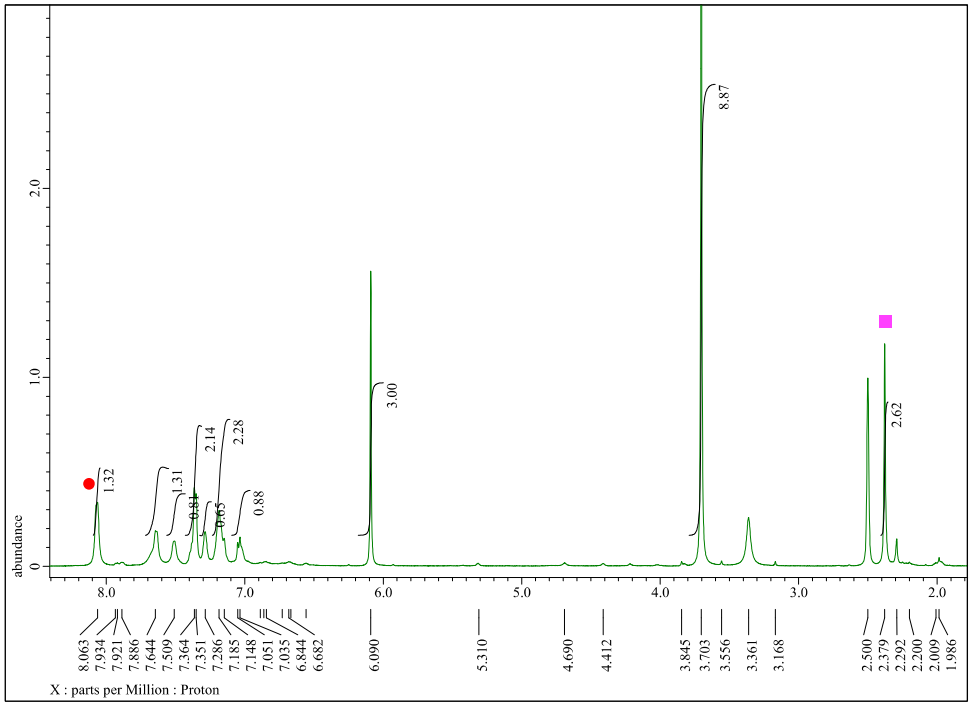

Figure 22. ^{1}H NMR Spectrum of the product mixture obtained by slow oxidation of a mixture of diimine **14c** and **3**. Critical peaks belonging to **12** are marked with a ● and those belonging to **17c** with a ■.

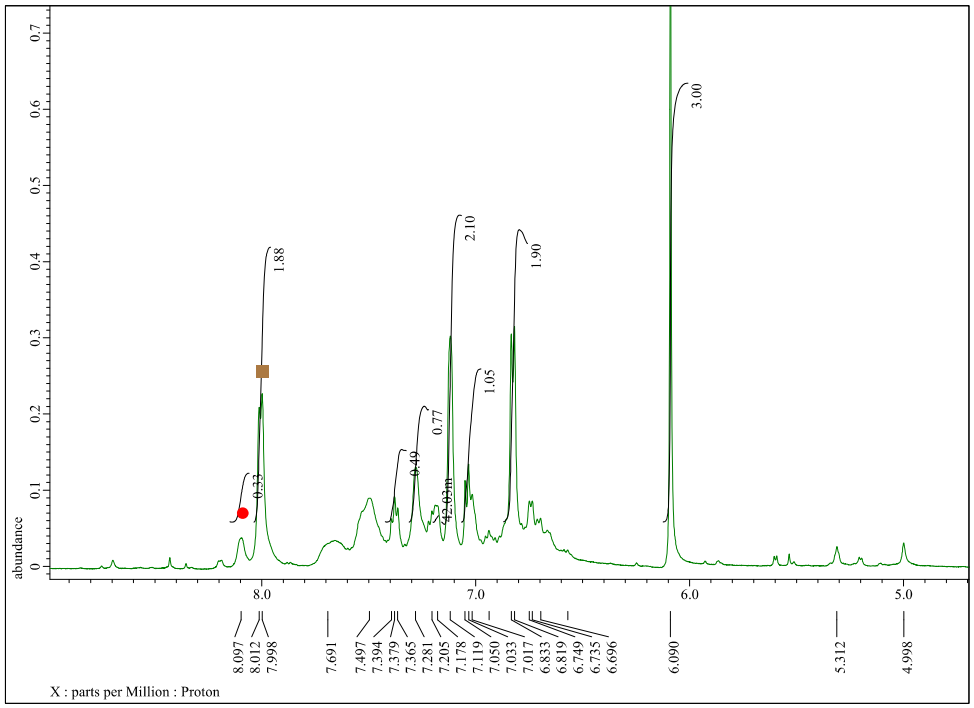

Figure 23. [1]H NMR Spectrum of the product mixture obtained by slow oxidation of a mixture of diimine **14d** and **3**. Critical peaks belonging to **12** are marked with a ● and those belonging to **17d** with a ■.

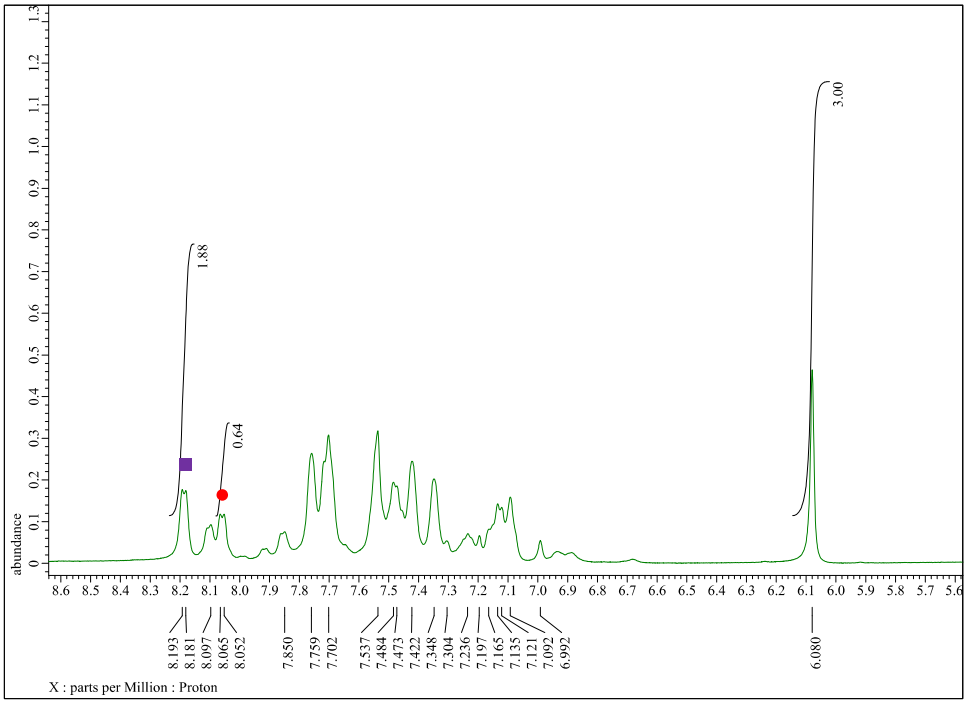

Figure 24. [1]H NMR Spectrum of the product mixture obtained by slow oxidation of a mixture of diimine **14e** and **3**. Critical peaks belonging to **12** are marked with a ● and those belonging to **6** with a ▲.

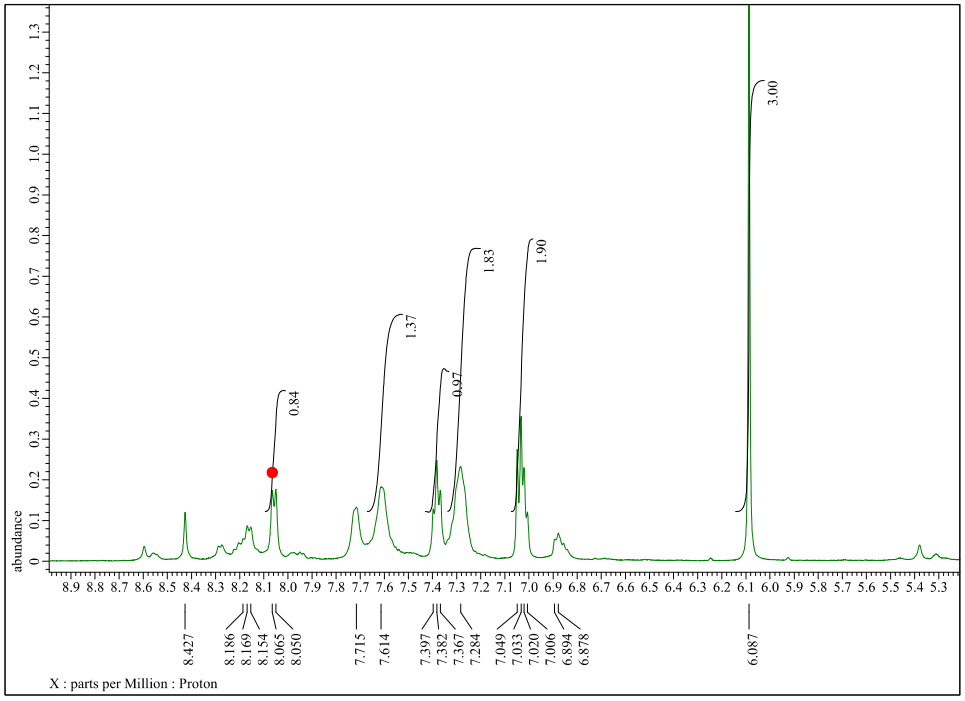

^{1}H NMR Spectra of Product Mixtures Obtained in Oxidations of 8 with 4

Figure 25. A segment of the ^{1}H NMR spectrum of the product mixture obtained by the oxidation of a mixture of diimine **8** and **4**. Critical peaks belonging to **12** are marked with a ●, those belonging to **6** with a ▲, and those of **13** with a ■. Iodine addition time: 1 min.

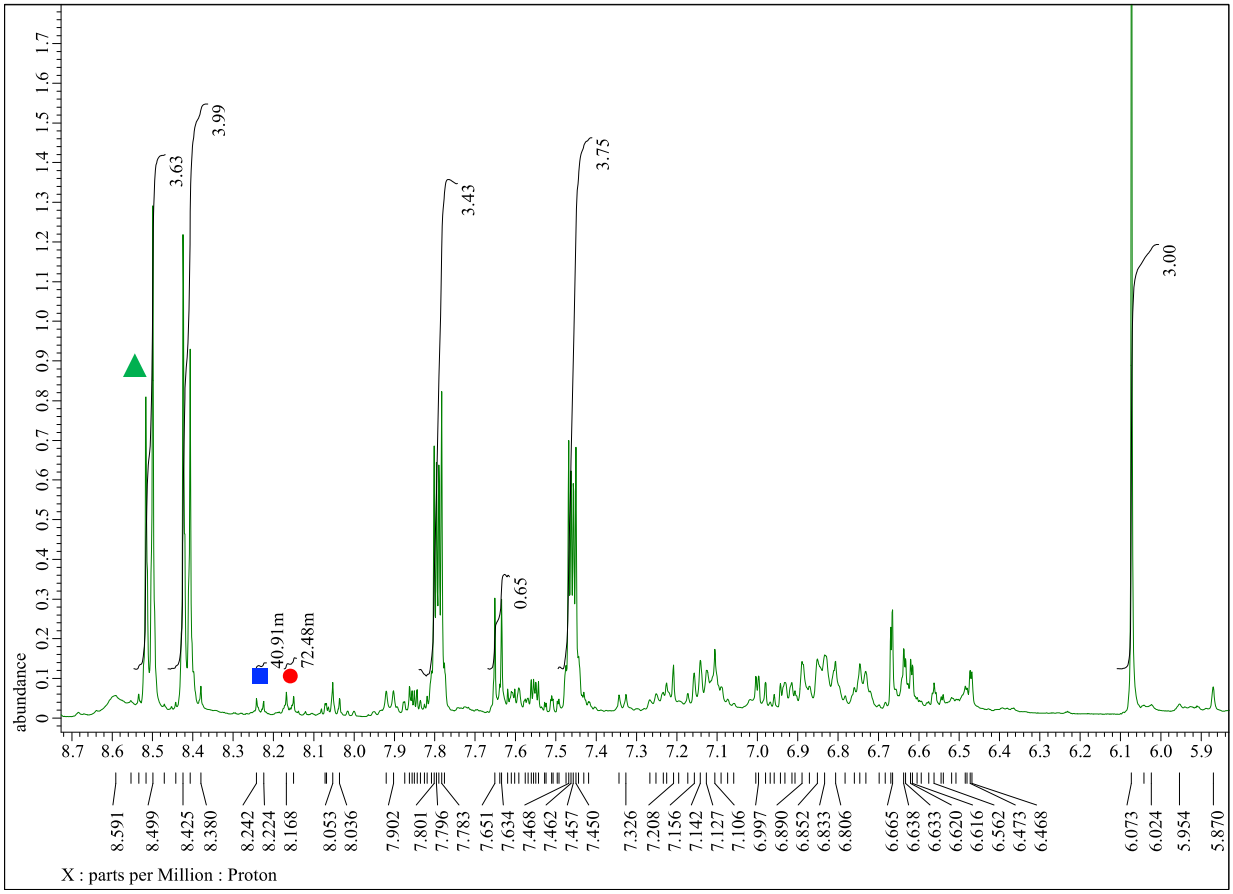

Figure 26. A segment of the ^{1}H NMR spectrum of the product mixture obtained by the oxidation of a mixture of diimine **8** and **4**. Critical peaks belonging to **12** are marked with a ●, those belonging to **6** with a ▲, and those of **13** with a ■. Iodine addition time: 1 h.

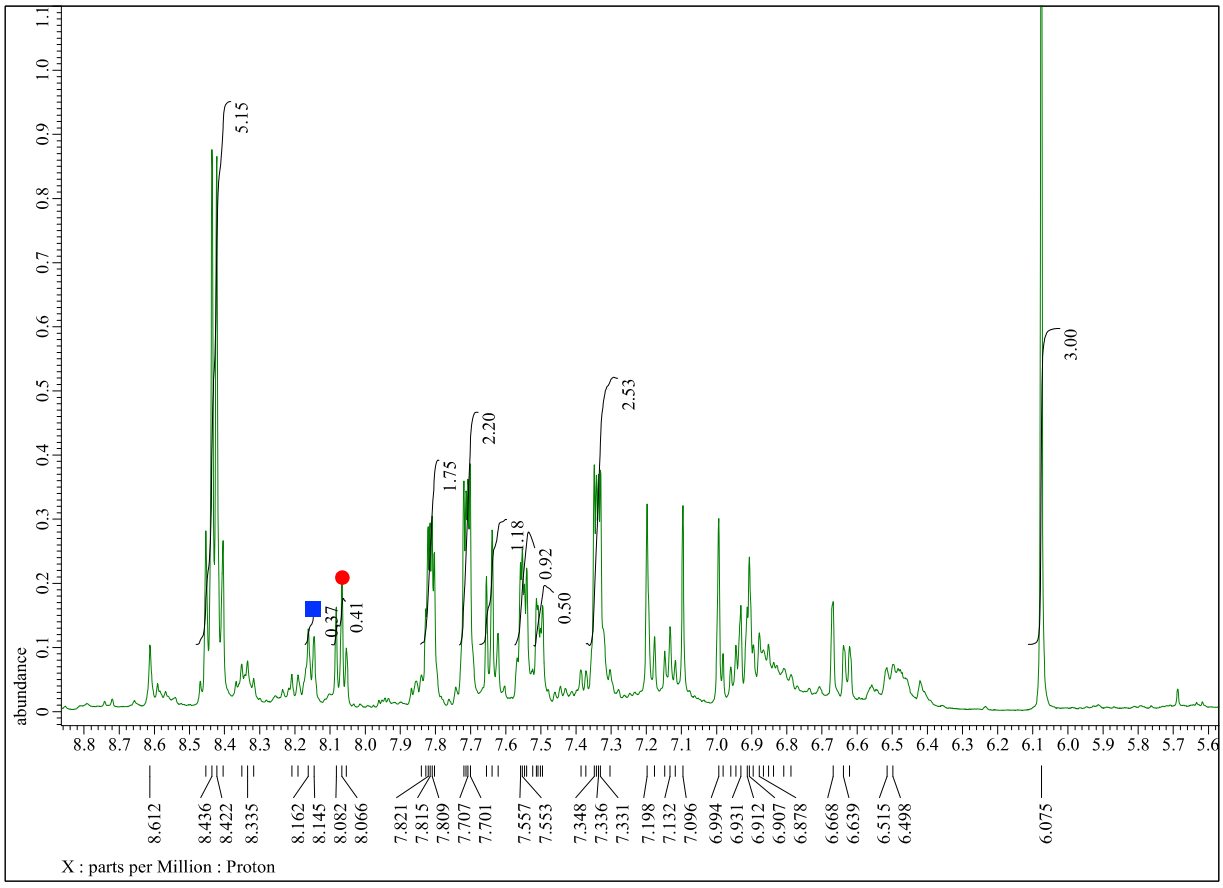

Figure 27. A segment of the ^{1}H NMR spectrum of the product mixture obtained by the oxidation of a mixture of diimine **8** and **4**. Critical peaks belonging to **12** are marked with a ●, those belonging to **6** with a ▲, and those of **13** with a ■. Iodine addition time: 2 h.

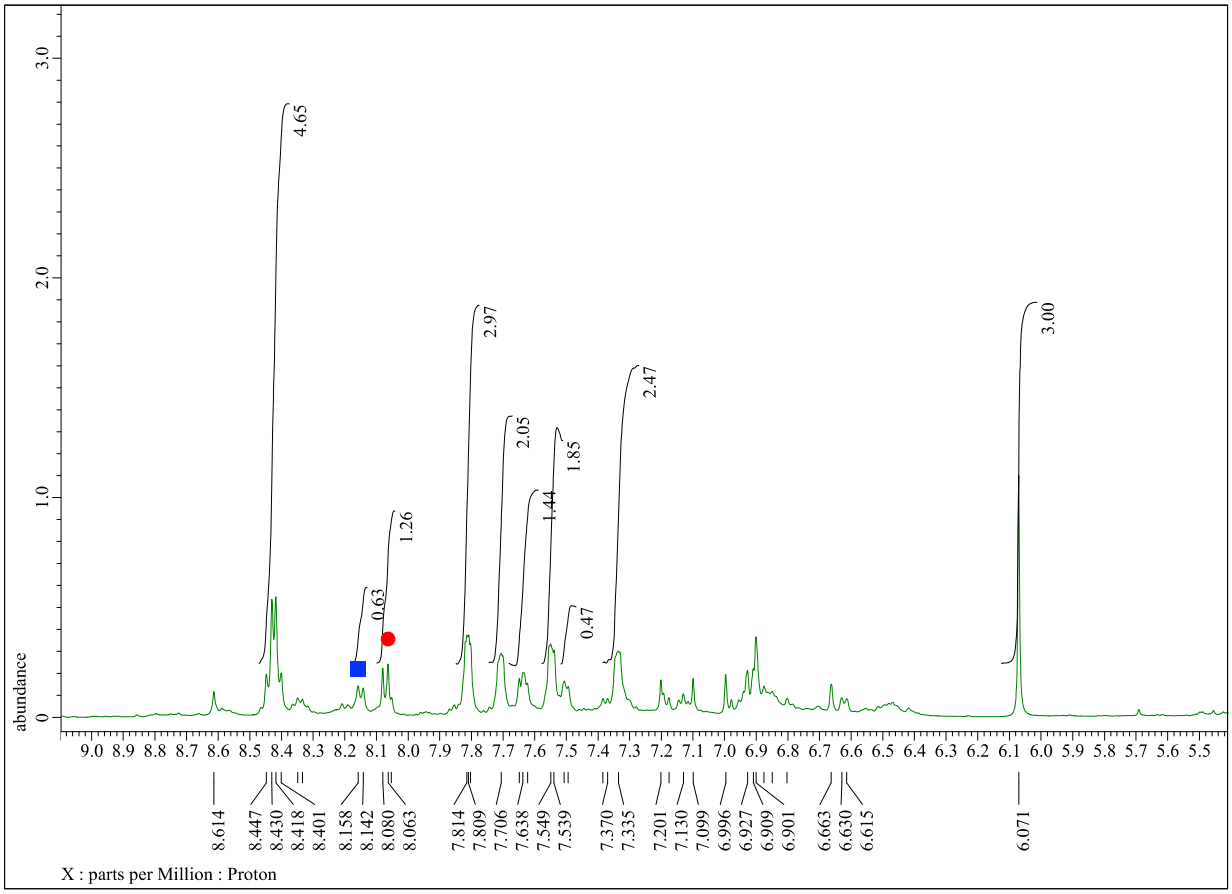

Figure 28. A segment of the ^{1}H NMR spectrum of the product mixture obtained by the oxidation of a mixture of diimine **8** and **4**. Critical peaks belonging to **12** are marked with a ●, those belonging to **6** with a ▲, and those of **13** with a ■. Iodine addition time: 3 h.

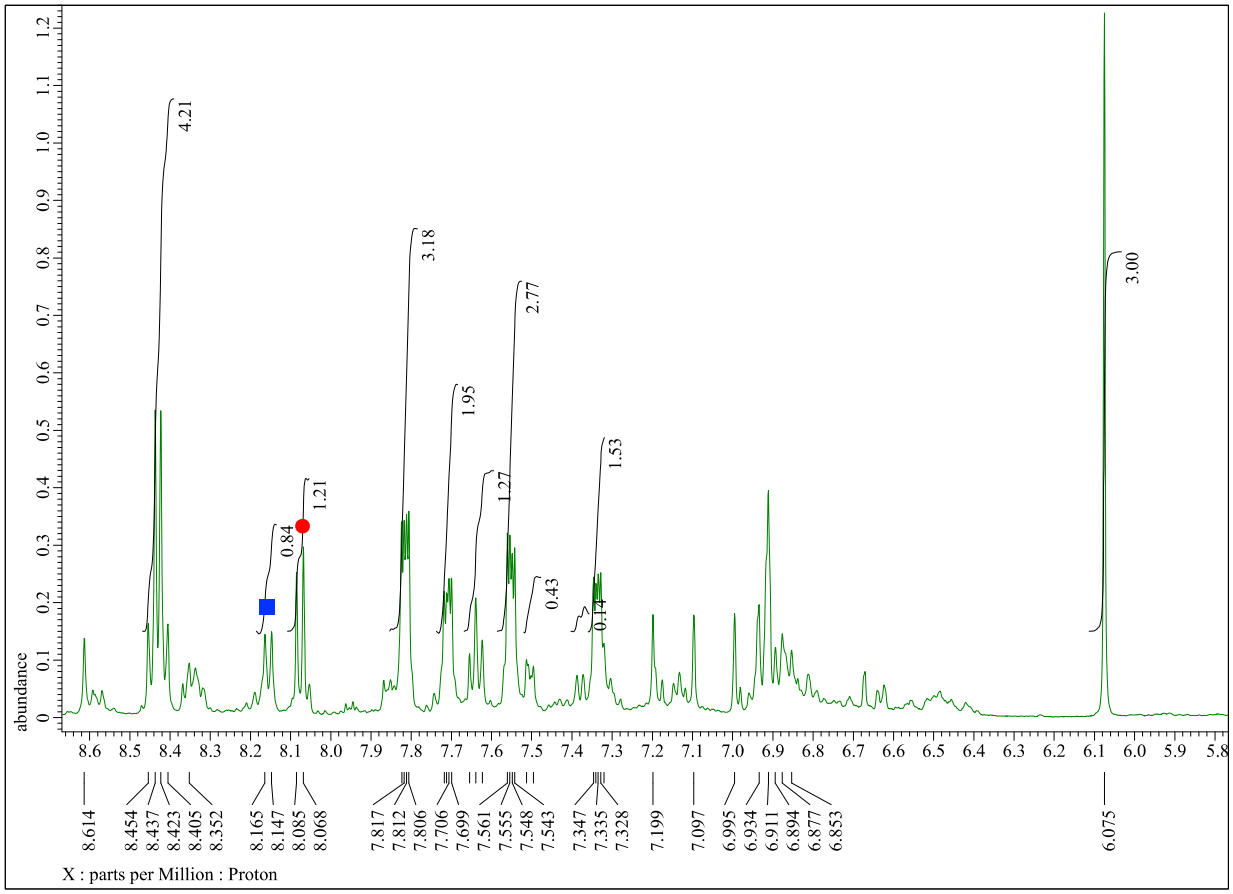

Figure 29. A segment of the ^{1}H NMR spectrum of the product mixture obtained by the oxidation of a mixture of diimine **8** and **4**. Critical peaks belonging to **12** are marked with a ●, those belonging to **6** with a ▲, and those of **13** with a ■. Iodine addition time: 4 h.

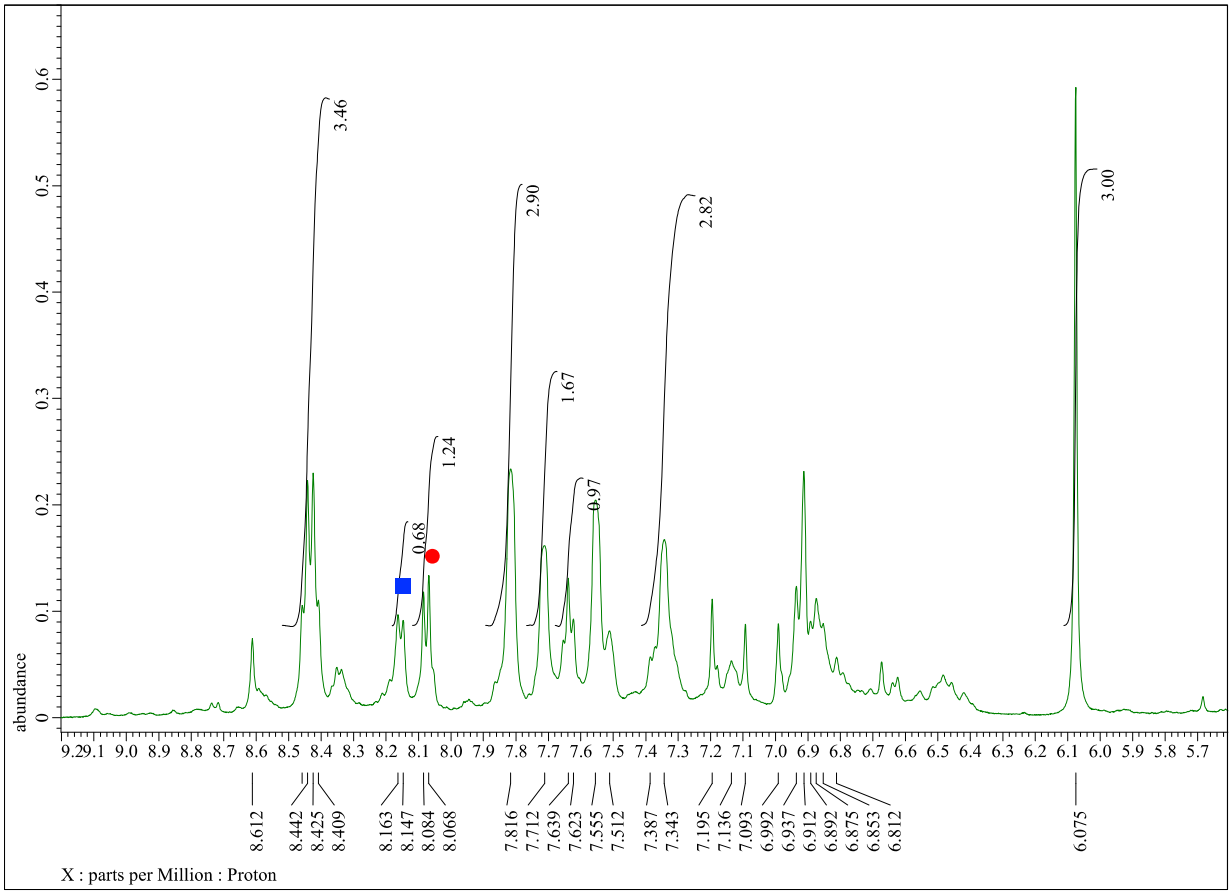

Figure 30. A segment of the ^{1}H NMR spectrum of the product mixture obtained by the oxidation of a mixture of diimine **8** and **4**. Critical peaks belonging to **12** are marked with a ●, those belonging to **6** with a ▲, and those of **13** with a ■. Iodine addition time: 5 h.

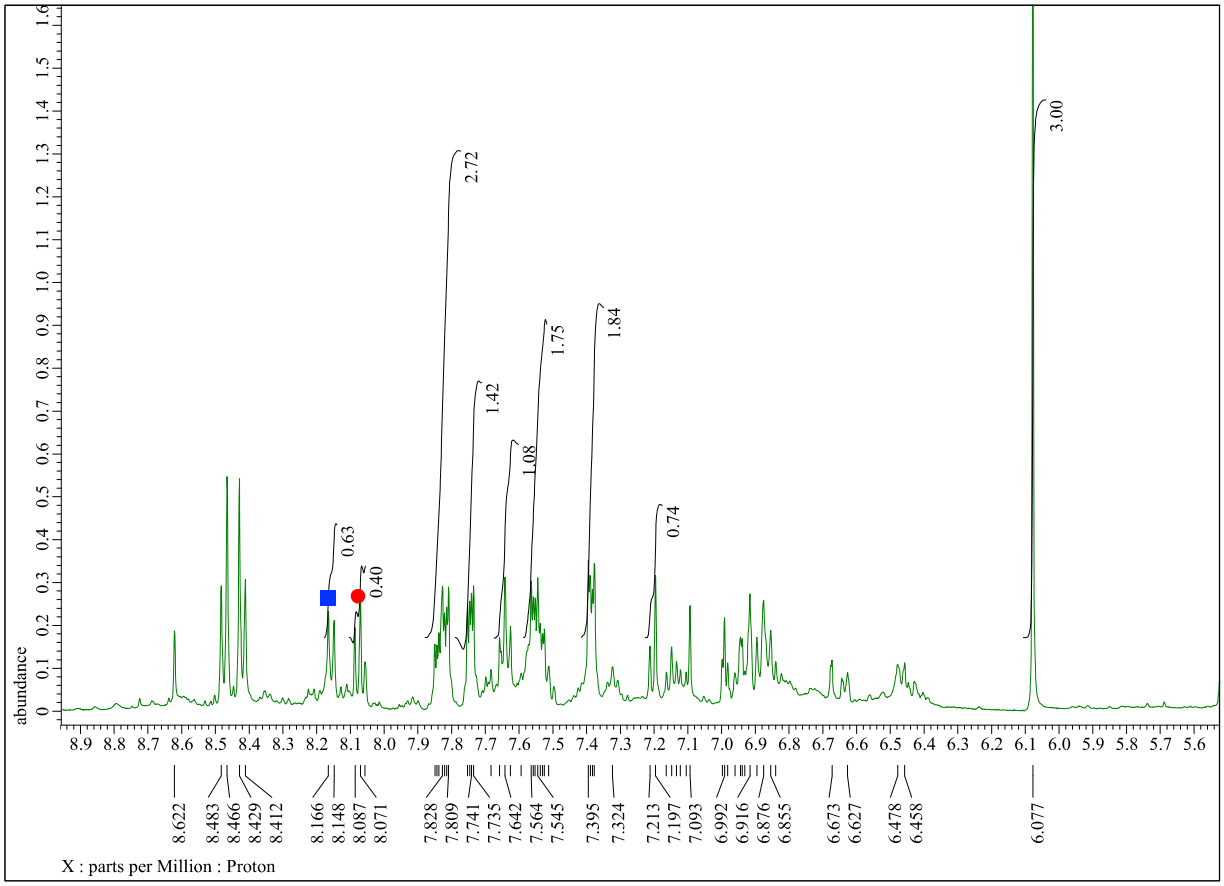

Figure 31. A segment of the ^{1}H NMR spectrum of the product mixture obtained by the oxidation of a mixture of diimine **8** and **4**. Critical peaks belonging to **12** are marked with a ●, those belonging to **6** with a ▲, and those of **13** with a ■. Iodine addition time: 6 h.

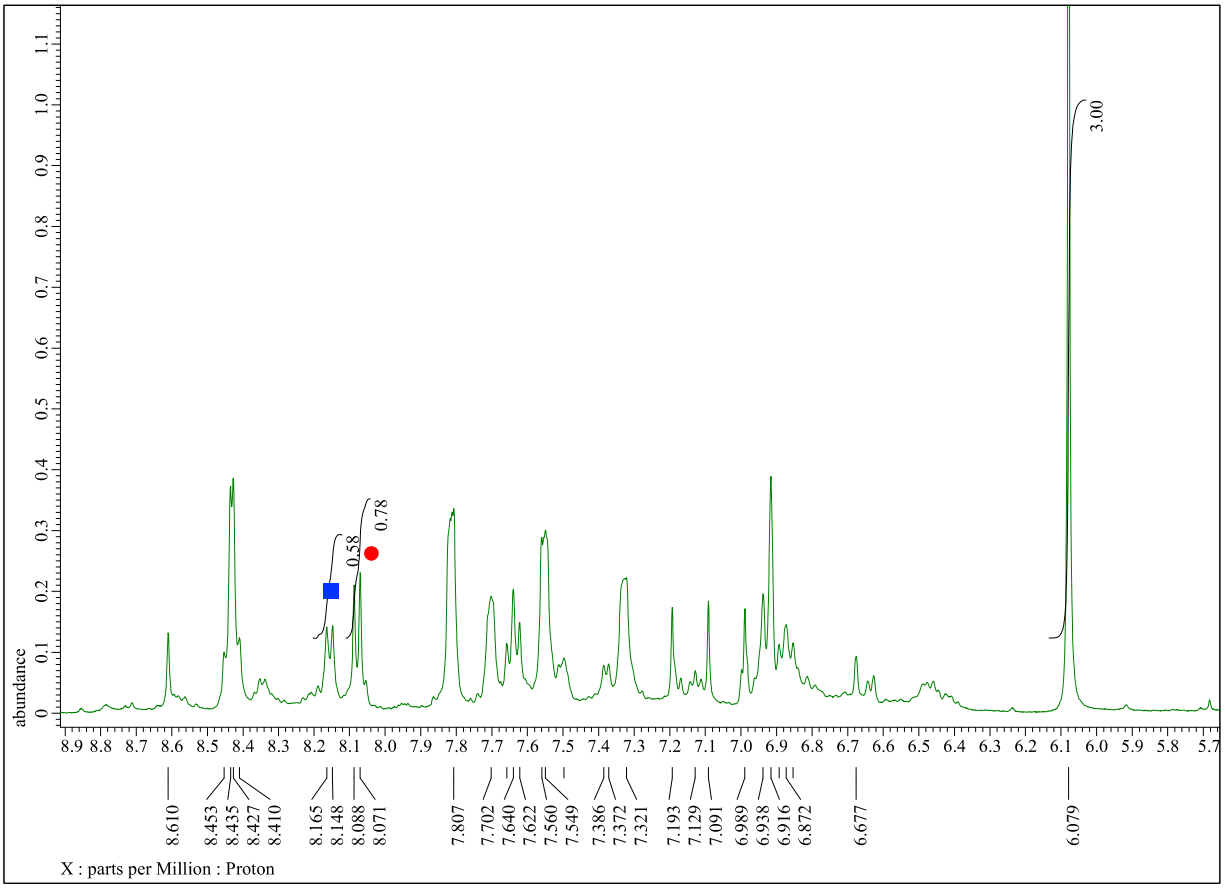

Figure 32. A segment of the ^{1}H NMR spectrum of the product mixture obtained by the oxidation of a mixture of diimine **8** and **4**. Critical peaks belonging to **12** are marked with a ●, those belonging to **6** with a ▲, and those of **13** with a ■. Iodine addition time: 24 h.

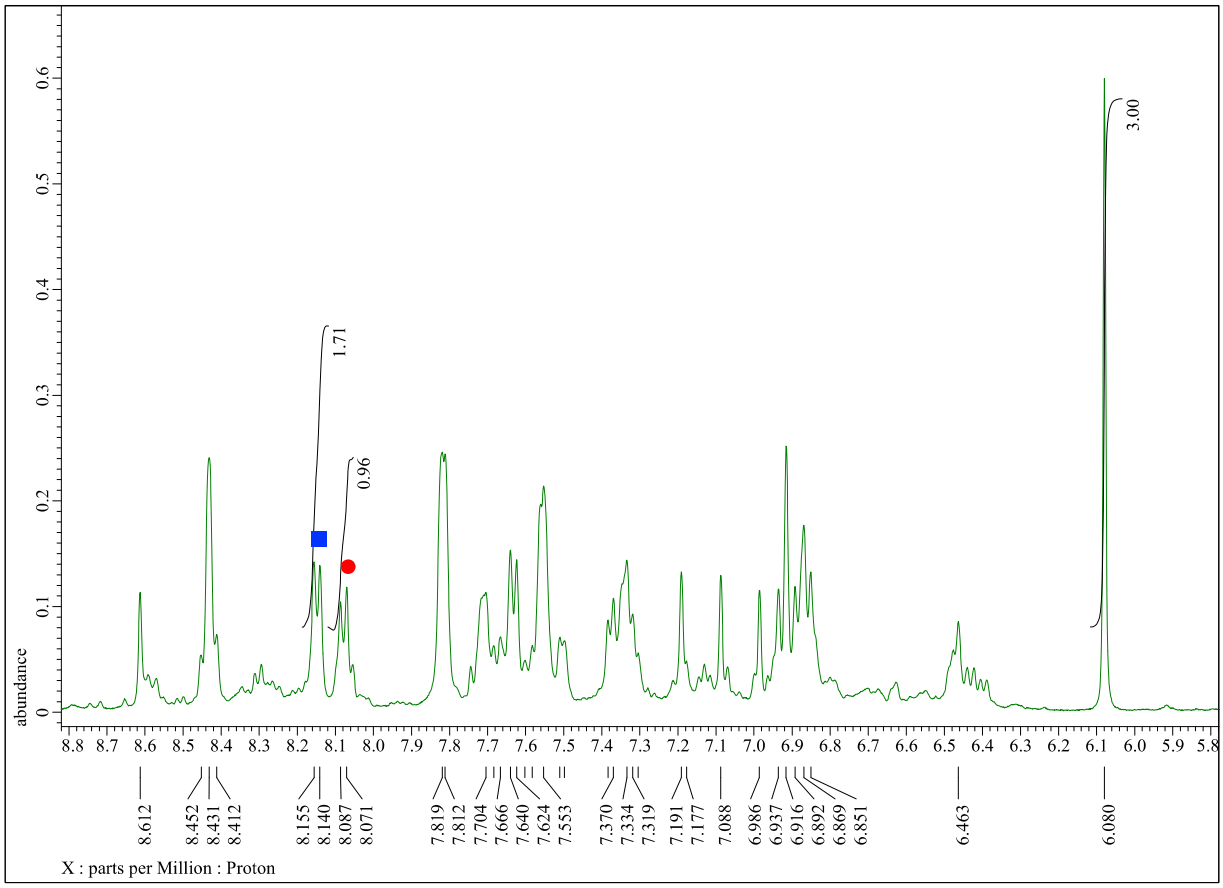

Figure 33. A segment of the ^{1}H NMR spectrum of the product mixture obtained by the oxidation of a mixture of diimine **8** and **4**. Critical peaks belonging to **12** are marked with a ●, those belonging to **6** with a ▲, and those of **13** with a ■. Iodine addition time: 120 h.

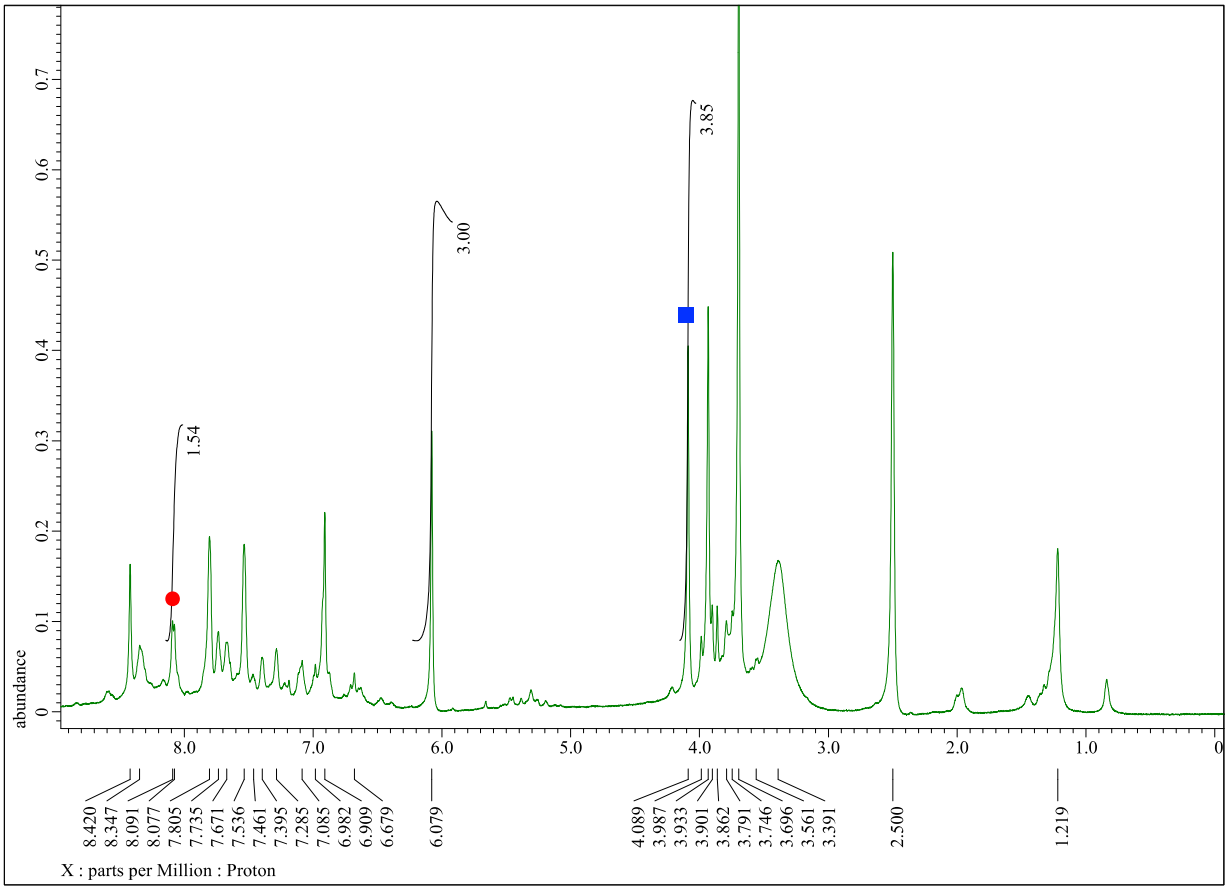

References

(1) Khier, N. B.; Amari, M.; Benkheira, F. Z.; Fodili, M.; Hoffmann. Selective Formation of 2-Amino-Iminoaldehyds: Synthesis of News Molecules of Benzimidazoles. *Org. Chem. Ind. J.* **2016**, *12*, 1–11.

(2) Vögtle, F.; Goldschmitt, E. Die Diaza-Cope-Umlagerung. *Chem. Ber.* **1976**, *109*, 1–40.

(3) Kim, H.; Nguyen, Y.; Yen, C. P.-H.; Chagal, L.; Lough, A. J.; Kim, B. M.; Chin, J. Stereospecific Synthesis of *C*2 Symmetric Diamines from the Mother Diamine by Resonance-Assisted Hydrogen-Bond Directed Diaza-Cope Rearrangement. *J. Am. Chem. Soc.* **2008**, *130*, 12184–12191.

(4) Manzari-Mogharabi, M.; Kiani, M.; Aryancjad, S.; Imanparast, S.; Amini, M.; Faramarzi, M. A. A Magnetic Heterogeneous Biocatalyst Composed of Immobilized Laccase and 2,2,6,6-Tetramethylpiperidine-1-oxyl (TEMPO) for Green One-Pot Cascade Synthesis of 2-Substituted Benzimidazole and Benzoxazole Derivatives under Mild Reaction Conditions. *Adv. Synth. Catal.* **2018**, *360*, 3563–3571.

(5) Hsu, C.-W.; Miljanić, O. Š. Kinetically Controlled Simplification of a Multiresponsive [10×10] Dynamic Imine Library. *Chem. Commun.* **2016**, *52*, 12357–12359.

(6) Osowska, K.; Miljanić, O. Š. Oxidative Kinetic Self-Sorting of a Dynamic Imine Library. *J. Am. Chem. Soc.* **2011**, *133*, 724–727.

(7) Samanta, S.; Das, S.; Biswas, P. Photocatalysis by 3,6-Disubstituted-s-Tetrazine: Visible-Light Driven Metal-Free Green Synthesis of 2-Substituted Benzimidazole and Benzothiazole. *J. Org. Chem.* **2013**, *78*, 11184–11193.